




Universidad de Concepción  
Dirección de Postgrado  
Facultad de Ingeniería - Programa de Magíster en Ciencias de la Ingeniería con  
mención en Ingeniería Eléctrica



## **Non-Invasive Monitoring System of Physiological Variables**

Tesis para optar al grado de Magíster en Ciencias de la Ingeniería con  
mención en Ingeniería Eléctrica

JAVIER ANTONIO PATRICIO CHÁVEZ CERDA  
CONCEPCIÓN-CHILE  
2017

Profesor Guía: Esteban Pino Quiroga  
Dpto. de Ingeniería Eléctrica, Facultad de Ingeniería  
Universidad de Concepción

# Non-Invasive Monitoring System of Physiological Variables

**Javier Antonio Patricio Chávez Cerda**

becario Conicyt

Presentada en Cumplimiento Parcial de los  
Requerimientos del Grado de  
Magíster en Ciencias de la Ingeniería  
con mención en  
Ingeniería Eléctrica

de la

Dirección de Postgrado

de la

UNIVERSIDAD DE CONCEPCIÓN, CHILE



Marzo, 2017

# Non-Invasive Monitoring System of Physiological Variables

© Javier Antonio Patricio Chávez Cerda, 2017



## Resumen

### Sistema de Monitoreo No Invasivo de Variables Fisiológicas

Javier Chávez Cerda, MSc.

Universidad de Concepción, 2017

Esta tesis presenta un sistema de monitoreo no invasivo de variables fisiológicas. El sistema utiliza sensores de presión montados en una silla, los cuales capturan actividad cardíaca y respiratoria.

A partir de las señales adquiridas, se desarrollaron algoritmos para calibrar el sistema, calcular umbrales y ajustar la ganancia del sistema, algoritmos para estimar la calidad de la señal cardíaca y respiratoria adquirida, algoritmos para calcular la frecuencia cardíaca y frecuencia respiratoria a partir de las señales y algoritmos de diagnóstico con el objetivo de monitorear y generar alarmas ante anomalías.

Se midieron a 34 personas sanas en un ambiente de laboratorio, las cuales realizaron una secuencia de instrucciones para determinar el efecto de la posición en el sensor. También fueron medidos luego de realizar ejercicio físico con el objetivo de validar alarmas de frecuencia cardíaca y los algoritmos de estimación de calidad de la señal. Además, se midieron 24 personas que padecían fibrilación auricular (AF) en un hospital, con el objetivo de validar alarmas de ritmo cardíaco. Finalmente se simularon casos de actividad cardíaca con diferentes niveles de ruido, en donde se evaluó el error de estimación de frecuencia cardíaca y el retardo en la generación de alarmas y se compararon estos valores con lo indicado en el estándar ANSI/AAMI para monitores de actividad cardíaca.

Se procedió a validar, en forma off-line, los algoritmos de estimación de calidad de las señales, la estimación de la frecuencia cardíaca, la detección de apneas en la señal respiratoria y las alarmas. Los resultados arrojaron que la mejor postura para

monitorear las señales es la de estar sentado apoyado en el respaldo con un error de estimación de frecuencia cardíaca de  $-0.41 \pm 3.76$  BPM y con una medición efectiva del 51 %. La estimación de calidad de la señal de balistocardiograma arrojó un 95 % de sensibilidad para detectar ruido. En cuanto a la señal respiratoria, el algoritmo para estimar una mala calidad de la señal arrojó un 87 % de sensibilidad.

En cuanto al diagnóstico de apneas se obtuvo un 86 % de sensibilidad y un 76 % de especificidad. Con respecto al diagnóstico de arritmias, el algoritmo obtuvo un 89.7 % de precisión en la condición de reposo, un 85.4 % de precisión después del ejercicio y un 73 % en el diagnóstico de ritmo cardíaco.

En cuanto a las simulaciones, se comprobó que el algoritmo de diagnóstico de actividad cardíaca es capaz de medir un rango de frecuencias de 30 a 300 bpm, además de alertar dentro de los rangos de tiempo estándares para casos de asístole y taquicardia.

Finalmente los algoritmos fueron probados en tiempo real en un computador de placa única, los cuales cumplieron con los requerimientos de tiempo de ejecución, lo que indica que los algoritmos pueden ser implementados en tiempo real utilizando una Raspberry Pi 3, la cual se comunica por WiFi a un computador principal para reportar las alarmas.

Se concluye que el algoritmo es capaz de generar alarmas a partir del uso de sensores no invasivos a través de un monitoreo en tiempo real, sin afectar la comodidad del paciente.

## Abstract

### Non-Invasive Monitoring System of Physiological Variables

Javier Chávez Cerda, MSc.

Universidad de Concepción, 2017

This thesis presents a noninvasive monitoring system of physiological variables. The system uses pressure sensors mounted on a chair, which capture cardiac and respiratory activity.

From the acquired signals, algorithms were developed to calibrate the system, calculate thresholds and adjust the gain of the system, algorithms to estimate the quality of the acquired cardiac and respiratory signal, algorithms to calculate the heart rate and respiratory rate from the signals and diagnostic algorithms with the goal of monitoring and generating alarms against anomalies.

Thirty-four healthy subjects were measured in a laboratory environment, who performed a sequence of instructions to determine the effects of posture on the sensor. They were also measured after physical exercise in order to validate heart rate alarms and quality estimation algorithms. In addition, 24 people who had atrial fibrillation (AF) were measured in a hospital, in order to validate heart rhythm alarms. Finally, cases of cardiac activity with different noise levels were simulated, where the heart rate estimation error and the generation of alarms delay were evaluated and compared with the ANSI/AAMI standard for activity monitors cardiac.

The algorithms of estimation of signal quality, estimation of heart rate, apneas detection in respiratory signal and alarms were validated off-line. The results showed that the best posture to monitor the signals is sitting on backrest with a heart rate estimation error of  $-0.41 \pm 3.76$  BPM and an effective measurement of 51 %. The quality estimation of the ballistocardiogram signal had a 95 % sensitivity to detect

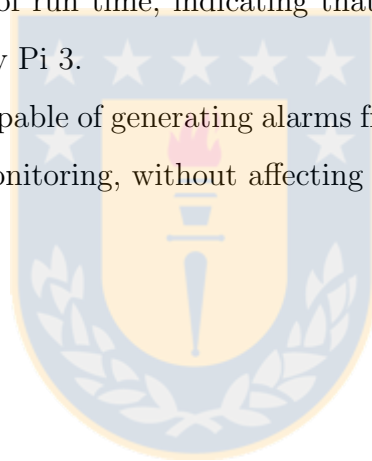
noise. As for the respiratory signal, the algorithm for estimating poor signal quality had a 87 % sensitivity.

For the diagnosis of apneas, a 86 % sensitivity and 76 % specificity was obtained. Regarding the diagnosis of arrhythmias, the algorithm obtained 89.7 % accuracy in the rest condition, 85.4 % accuracy after exercise and 73 % in the heart rhythm diagnosis.

For the simulations, the cardiac activity diagnostic algorithm is able to measure a frequency range of 30 to 300 bpm. In addition to alerting within the standard time ranges for cases of asystole and tachycardia.

Finally, the algorithms were tested in real time on a single-board computer, which met the requirements of run time, indicating that they can be implemented in real time using a Raspberry Pi 3.

The algorithm is capable of generating alarms from the use of non-invasive sensors through a real-time monitoring, without affecting the comfort of the patient.



A mi abuelo y a mi tío QEPD



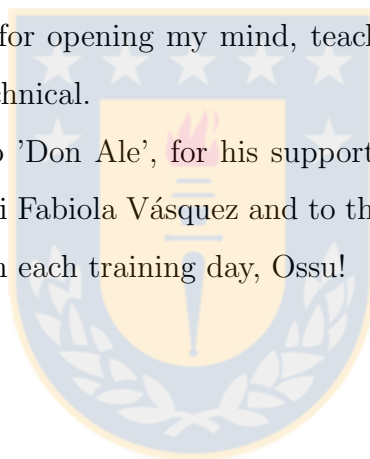


## Acknowledgements

I thank to my parents Claudia and Mauro and my brothers Gonzalo and Jorge for all their love and unconditional support. To my friends Ricardo, Alejandra, Daniela, Constanza, Miguel, Britam and Enrique for their friendship in all these years of university.

I am grateful to professor Esteban Pino for the support, confidence and patience provided in all these years of work. I am also grateful to professor Pablo Aqueveque and professor Pamela Guevara for his advices and suggestions during the development of this thesis. I also thank to Dr. Lecannelier and all the cardiology team who helped me to carry out the measurements at the hospital. I also thanks to César Hidalgo and Carlos Rodríguez for opening my mind, teaching me that this kind of projects are beyond just the technical.

I specially thank to 'Don Ale', for his support, patient and life's advices. Also, special thanks to Sensei Fabiola Vásquez and to the Dojo Shynkiokushin Concepción for the life teachings on each training day, Ossu!



### **Acknowledgements to CONICYT and FONDEQUIP**

This thesis has been supported by CONICYT-PCHA/Magíster Nacional/2014-2214548. Also, this work has been supported by research grant FONDEQUIP EQM-150114.



# Contents

<b>Resumen</b>	<b>i</b>
<b>Abstract</b>	<b>iii</b>
<b>List of Figures</b>	<b>xi</b>
<b>List of Tables</b>	<b>xii</b>
<b>1 Introducción</b>	<b>1</b>
1.1 Problemática Global . . . . .	1
1.2 Hipótesis . . . . .	2
1.3 Objetivos . . . . .	3
1.3.1 Objetivo General . . . . .	3
1.3.2 Objetivos Específicos . . . . .	3
1.4 Temario . . . . .	3
<b>2 Introduction</b>	<b>5</b>
2.1 Global Issues . . . . .	5
2.2 Hypothesis . . . . .	6
2.3 Goals . . . . .	6
2.3.1 Main Goal . . . . .	6
2.3.2 Specific Goals . . . . .	7
2.4 Thesis Overview . . . . .	7
<b>3 Background</b>	<b>9</b>
3.1 Unobtrusive Sensors and Signal Preprocessing . . . . .	9
3.1.1 Unobtrusive sensors . . . . .	9
3.1.2 Signal Preprocessing . . . . .	13
3.2 Algorithms . . . . .	14
3.2.1 Heartbeats Detection . . . . .	14
3.2.2 Respiratory Cycles Detection . . . . .	15
3.2.3 Noise Detection . . . . .	16

3.3	Alarms Criteria . . . . .	16
3.4	Discussion . . . . .	17
<b>4</b>	<b>System Description</b>	<b>19</b>
4.1	System Stages . . . . .	19
4.1.1	Unobtrusive sensors . . . . .	19
4.1.2	Analog Circuit . . . . .	20
4.1.3	Analog to Digital Conversion (ADC) . . . . .	21
4.1.4	Single Board Computer (SBC) . . . . .	22
4.1.5	Wireless Communications . . . . .	23
4.2	Power Supply . . . . .	24
<b>5</b>	<b>Algorithms and Signal Processing</b>	<b>25</b>
5.1	Calibration Stage . . . . .	25
5.2	BCG signal processing . . . . .	27
5.2.1	Peak Detection . . . . .	27
5.2.2	Noise Estimation . . . . .	30
5.2.3	BCG Diagnosis Algorithm . . . . .	32
5.3	Respiration Signal Processing . . . . .	37
5.3.1	Respiration Cycle detection . . . . .	37
5.3.2	Noise Signal Detection . . . . .	38
5.3.3	Respiration Diagnosis Algorithm . . . . .	39
<b>6</b>	<b>Measurements and Simulations</b>	<b>42</b>
6.1	Measurements . . . . .	42
6.1.1	Laboratory Measurements . . . . .	42
6.1.2	Hospital Measurements . . . . .	44
6.2	Signals Simulations . . . . .	44
6.2.1	ANSI/AAMI EC13:2002 . . . . .	45
6.2.2	Synthetic Signals . . . . .	45
<b>7</b>	<b>Results</b>	<b>48</b>
7.1	Cardiac Activity . . . . .	48
7.1.1	Position Accuracy . . . . .	48
7.1.2	Noise Detection Accuracy . . . . .	49
7.1.3	Diagnosis Accuracy . . . . .	49
7.1.4	Simulations Results . . . . .	51
7.2	Respiration Activity . . . . .	52
7.2.1	Noise Detection Results . . . . .	52
7.2.2	Apnea Detection . . . . .	54
7.3	Raspberry Performance . . . . .	54
7.3.1	Timing analysis . . . . .	55

7.3.2	Temperature . . . . .	55
7.3.3	CPU usage . . . . .	56
7.3.4	Memory usage . . . . .	56
7.3.5	Power Requirements . . . . .	57
<b>8</b>	<b>General Discussion and Conclusions</b>	<b>58</b>
8.1	Discussion . . . . .	58
8.2	Conclusions . . . . .	60
<b>9</b>	<b>Discusión General y Conclusiones</b>	<b>62</b>
9.1	Discusión . . . . .	62
9.2	Conclusiones . . . . .	64
<b>10</b>	<b>Publications</b>	<b>66</b>
10.1	ISI Paper Submitted . . . . .	66
10.2	Conferences . . . . .	66
<b>Bibliography</b>		<b>68</b>



# List of Figures

3.1	Simplified model structure of EMFi and PVDF Sensors . . . . .	11
3.2	Electrocardiogram and Ballistocardiogram signals. . . . .	12
3.3	BCG signal with respiration baseline. . . . .	13
4.1	General System . . . . .	20
4.2	Sensors on a chair . . . . .	21
4.3	Charge Amplifier . . . . .	22
4.4	FSR Circuit . . . . .	23
4.5	Raspberry Pi 3. . . . .	24
5.1	Calibration Flow Chart . . . . .	26
5.2	Multiple Smoothed Length Transform . . . . .	29
5.3	Neighbourhood Length Estimation . . . . .	30
5.4	Good Quality Signal . . . . .	31
5.5	Bad Quality Signal . . . . .	32
5.6	Histogram of periods SD . . . . .	33
5.7	Heart Rate Variability by Motion Artifact . . . . .	34
5.8	Flow Chart BCG Diagnosis Algorithm . . . . .	35
5.9	Respiration Algorithm Criteria . . . . .	38
5.10	Respiration quality . . . . .	39
5.11	Flow Chart Respiration Diagnosis . . . . .	40
6.1	Different positions for measurements . . . . .	43
6.2	Apneas Simulation . . . . .	44
6.3	Noisy BCG Simulation . . . . .	46
7.1	ROC curve of noisy respiration detection . . . . .	53
7.2	Timing Analysis . . . . .	54
7.3	Raspberry Resources . . . . .	55
7.4	Raspberry current demand . . . . .	56

# List of Tables

4.1	Raspberry Pi 3 Features . . . . .	23
5.1	Different Reports on Diagnoses Algorithm . . . . .	37
5.2	Respiration Diagnosis . . . . .	41
7.1	Number of discarded segments and HR error estimation for each position. . . . .	49
7.2	Noise Detection Accuracy . . . . .	49
7.3	Diagnosis Accuracy: Resting Condition . . . . .	50
7.4	Diagnosis Accuracy: After Exercise Condition . . . . .	50
7.5	Diagnosis Accuracy: Atrial Fibrillation . . . . .	51
7.6	HR error of each frequency . . . . .	52
7.7	General HR error estimation . . . . .	52
7.8	Delay simulation . . . . .	53
8.1	Material Costs . . . . .	60
9.1	Costos de los materiales . . . . .	64

# Acronyms

**AAMI** Association for the Advancement of Medical Instrumentation

**ADC** Analog-Digital Converter

**AF** Atrial Fibrillation

**ANSI** American National Standards Institute

**BCG** Ballistocardiogram

**BIH** Beth Israel Hospital

**BPM** Beat per minute

**CASEN** Caracterización Socioeconómica Nacional

**ECG** Electrocardiogram

**EMFi** Electro Mechanical Film

**FSR** Force Sensitive Resistor

**HC** Home Care

**HR** Heart Rate

**HRV** Heart Rate Variability

**I2C** Inter-Integrated Circuit





**IIR** Infinite Impulse Response

**INE** Instituta Nacional de Estadísticas

**IP** Internet Protocol

**LT** Length Transform

**MIT** Massachusetts Institute of Technology

**NSR** Normal Sinus Rhythm

**PVDF** Polyvinylidene fluoride

**QI** Quality Index

**ROC** Receiver Operating Characteristic

**RR** Respiratory Rate

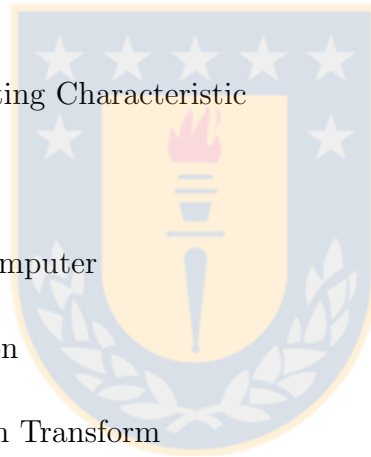
**SBC** Single Board Computer

**SD** Standard Deviation

**SLT** Smoothed Length Transform

**TCP** Transmission Control Protocol

**VAR** Variance



# Chapter 1

## Introducción

En este capítulo se introduce el problema global que motiva el desarrollo de esta tesis, la hipótesis de ésta y sus objetivos. Luego, se describe como está organizado el trabajo en sus diferentes capítulos.

### 1.1 Problemática Global

La enfermedad cardíaca es la principal causa de muerte en todo el mundo y está fuertemente relacionada con el envejecimiento de la población, la cual crece rápidamente cada década. De hecho, para el año 2050 se espera que la población mundial de adultos mayores se triplique [1].

En Chile, según la encuesta CASEN 2013, hay 2.885.157 adultos mayores que representan el 16,7 % de la población chilena y el 6,7 % tienen una severa dependencia funcional. Además, según estudios del Instituto Nacional de Estadísticas (INE) de 2007, la población de más edad alcanzará a la población de jóvenes menores de 15 años en el año 2025, lo que confirma el envejecimiento de la población chilena.

Eso significa que en el futuro, la población aumentará los controles y visitas a los establecimientos de salud. El aumento de los adultos mayores con grave dependencia funcional hace que la atención médica en el hogar sea necesaria.

Uno de los principales problemas que existen en los hospitales chilenos es en las salas de espera, donde los pacientes deben esperar largas horas para ser atendidos por un especialista. Han existido casos en los que los pacientes han muerto en espera de atención, donde no hubo advertencias de aquello [2–5].. Con respecto a las personas con dependencia funcional, "HomeCare" (HC) es una alternativa de salud en el hogar, entregando un ambiente psicológico más humanizado. Sin embargo, los pacientes tratados en el sistema de HC se caracterizan por la necesidad de atención permanente y vigilancia activa por parte del personal a cargo o familiares.

Esto lleva a la necesidad de un sistema de monitoreo de variables fisiológicas como la actividad cardíaca y respiratoria, que alerte anomalías para un cuidado oportuno. Aunque existen métodos para medir estas variables como el electrocardiograma y bandas respiratorias, éstas interfieren con la comodidad del paciente.

En las últimas décadas, investigaciones han desarrollado diferentes técnicas para medir la actividad cardíaca y respiratoria de manera no invasiva. Estas tienen la ventaja de no incomodar al paciente y que son fáciles de utilizar, ya que el paciente sólo necesita apoyarse en los sensores a ser monitoreado.

Esta tesis presenta un sistema de monitoreo, que emite alarmas a partir de señales obtenidas por sensores no invasivos con el objetivo de resolver los problemas descritos.

## 1.2 Hipótesis

A partir de la información de latidos cardíacos y movimientos respiratorios, obtenidos mediante el uso de sensores no invasivos, es posible generar alarmas oportunas que apoyen el cuidado del paciente.

## 1.3 Objetivos

### 1.3.1 Objetivo General

Diseñar e implementar un sistema de alarmas oportunas ante anomalías cardíacas y respiratorias obtenidas de sensores no invasivos de presión.

### 1.3.2 Objetivos Específicos

- Investigar e implementar criterios para la detección de anomalías más comunes de la actividad cardíaca y respiratoria.
- Capturar señales cardíacas con ajuste de ganancia automática para diferentes personas.
- Implementar algoritmos de evaluación de la información cardíaca y respiratoria en tiempo real en un computador de placa única (SBC).
- Implementar algoritmos de detección de señales de baja calidad en tiempo real, para evitar generar falsas alarmas.
- Desarrollar e implementar un software en un computador principal que se comunique con el SBC, el cuál actuará como servidor y recibirá las alarmas emitidas por los clientes.
- Realizar simulaciones de señales, pruebas a voluntarios y a pacientes para probar la efectividad del sistema.

## 1.4 Temario

Este trabajo está organizado en 7 capítulos. El capítulo 1 presenta la problemática global que motiva este trabajo de investigación, la hipótesis de ésta y sus objetivos.

En el capítulo 2 se revisa el estado del arte del desarrollo de sistemas no invasivos, los sensores utilizados, los algoritmos de preprocesamiento y análisis, detección de ruido y el criterio de alarmas.

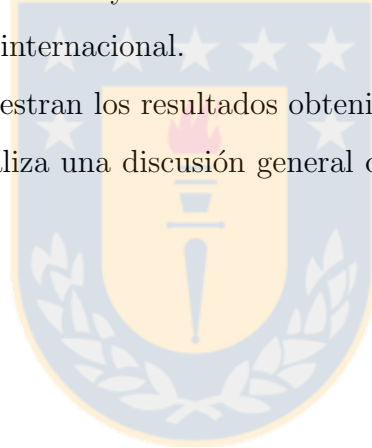
El capítulo 3 describe el sistema de adquisición, donde se describen los sensores seleccionados y el hardware para acondicionar y adquirir las señales. Luego se describe como se energiza el sistema.

El capítulo 4 detalla los algoritmos propuestos para el pre-procesamiento y obtención de parámetros fisiológicos a partir de las señales adquiridas, y los criterios para realizar un diagnóstico con estos valores.

El capítulo 5 describe la metodología de las mediciones realizadas a sujetos de prueba para validar el sistema y las simulaciones realizadas para comparar los resultados con un estándar internacional.

El capítulo 6 se muestran los resultados obtenidos.

El capítulo 7 se realiza una discusión general del trabajo y se presentan las conclusiones.



# Chapter 2

## Introduction

This chapter introduces the global problem that motivates the development of this thesis, its hypothesis and its objectives. Then, it describes how this work is organized in its different chapters.

### 2.1 Global Issues

Heart disease is the main cause of death worldwide and is strongly related to the ageing population, which is growing rapidly every decade. In fact, by the year 2050 the worldwide population of older adults is expected to triple [1]. In Chile, according to the CASEN 2013 survey, there are 2.885.157 older adults representing 16.7% of the Chilean population and 6.7% have a severe functional dependency. Also, according to 2007 studies by the National Institute of Statistics (INE) the older population will reach the population of young people under 15 years old in 2025, confirming the ageing of the Chilean population.

This means that in the future, population will increase controls and visits to health facilities and the increase of older adults with severe functional dependence makes medical care at home necessary.

One of the major problems that exists in Chilean hospitals is in waiting rooms,

where patients must wait long hours to be seeing by a specialist. There have been cases where patients have died waiting for care, where there were no warnings of that [2–5]. Regarding older people with functional dependency, "HomeCare" (HC) is a health care alternative at home, providing a more humanized psychological environment. However, the patients treated with HC systems are characterized by the need for permanent care and active surveillance by the staff in charge or their relatives.

This leads to the need for a monitoring system of physiological variables such as cardiac and respiratory activity, that alarms anomalies for timely care. Although there are methods to measure these variables, like electrocardiogram and respiratory bands, but they interfere with the patient's comfort.

In the last decades, research has developed different techniques for measuring cardiac and respiratory activity in a non-invasive way, which are not uncomfortable and are simple to use, since the patient only needs to lean on the sensors to be monitored.

This thesis presents a monitoring system that emits alarms from signals obtained by non-invasive sensors, with the aim of solving the problems described.

## **2.2 Hypothesis**

It is possible to generate a timely alarm that supports patient care, from the information of heartbeats and respiratory movements, obtained through the use of non-invasive pressure sensors.

## **2.3 Goals**

### **2.3.1 Main Goal**

Design and implement a timely alarm system for cardiac and respiratory anomalies obtained from non-invasive sensors.

### 2.3.2 Specific Goals

- Investigate and implement criteria for the detection of more common anomalies of cardiac and respiratory activity.
- Capture cardiac signals with automatic gain adjustments for different patient.
- Implement algorithms for evaluating cardiac and respiratory information in real time on a single board computer (SBC).
- Implement a low quality signal detection algorithm, in real time, to avoid generating false alarms.
- Develop and implement a software on a main computer that communicates with the SBC, which will act as server and receive the alarms issued by the clients.
- Perform simulations of signals, measure volunteers and patients to test the effectiveness of the system.

## 2.4 Thesis Overview

This work is organized into 7 chapters. Chapter 1 presents the global problem that motivates this research work, its hypothesis, and its objectives.

Chapter 2 reviews the state of the art in the development of non-invasive systems: sensors used, preprocessing and analysis algorithms, noise detection and alarm criteria.

Chapter 3 describes the acquisition system, which shows the selected sensors and the hardware for conditioning and acquiring the signals. It then describes how the system is energized.

Chapter 4 details the proposed algorithms for the preprocessing and obtaining of physiological parameters from the acquired signals, and the criteria for diagnosis using these values.



Chapter 5 describes the methodology of the measurements performed to test subjects, in order to validate the system and the simulations performed to compare the results with an international standard.

Chapter 6 shows the results obtained.

Chapter 7 conducts a general discussion of the work and presents the conclusions.



# Chapter 3

## Background

In this chapter, a bibliographical review is made on the non-invasive sensors used for measurement of cardiac and respiratory activity, and the hardware necessary for its conditioning. Then, the algorithms that have been used for signal pre-processing, algorithms for obtaining heart rate (HR) and respiratory rate (RR) from signals, and the algorithms of noise detection are reviewed. The alarm criteria used are then discussed. Finally, a general discussion of all these issues is made.

### 3.1 Unobtrusive Sensors and Signal Preprocessing

#### 3.1.1 Unobtrusive sensors

In recent years several works have been made on unobtrusive pressure sensors by measuring physiological signals such as breathing and cardiac activity. Preferred sensors are resistive, capacitive and piezoelectric sensors.

Resistive sensors are reliable and simple to use. They modify their resistance by applying force on them [6]. Force Sensing Resistor (FSR) has the characteristic that pressure applied on it decreases its resistance. FSR has many applications and is used in several works related with unobtrusive measurement. A system for polysomnog-

raphy screening was implemented using 24 FSR, arranged in 3 rows and 8 columns, positioned under a sheet, over a bed. This system captured the respiratory signal and body movements during the night. These captured signals were processed to obtain objective parameters of sleep quality. Also, the system can detect abnormalities like sleep apneas [7]. Other work used FSR to measure the pressure distribution of the subject on a wheelchair, in order to generate alarms when a pressure relief is needed. This is focused on the care of people with multiple sclerosis to prevent bedsores [8] [9].

Many electrical interfaces are proposed to transduce forces, for example a voltage divider, current-to-voltage converter, variable force threshold switch, adjustable buffers and many others [10]. The external circuit of the interface is also important because it configures the sensitivity of the interface.

Resistive sensors can capture respiration signals and measure pressure, but they do not have enough sensitivity to capture cardiac activity (besides the respiratory activity). Capacitive and piezoelectric sensors are capable of capturing this kind of signal.

One of the capacitive sensors is the electro-mechanical films (EMFi). EMFi sensors are composed of small bubbles of gas that separate charges over to plates (Fig. 3.1a). When a dynamic force is applied to this sensor, the separation of the electric charges is modified, causing a variation of charges between the electrodes of the sensor.

A typical piezoelectric sensor is the polyvinyl (PVDF). PVDF sensors have randomly oriented dipoles, which produce a zero internal net charge. When a force is applied to the sensor, the dipoles change their orientation, generating a net charge different from zero [11] (Fig. 3.1b).

Both sensors ,EMFi and PVDF, have different operating characteristics. They were compared applying dynamic normal and sliding forces on them. The research concluded that the EMFi sensors showed a high sensitivity to normal forces and a poor sensitivity to sliding forces. In contrast, PVDF sensors had a high sensitivity to slider forces and a lower sensitivity to normal forces. The EMFi has a normal

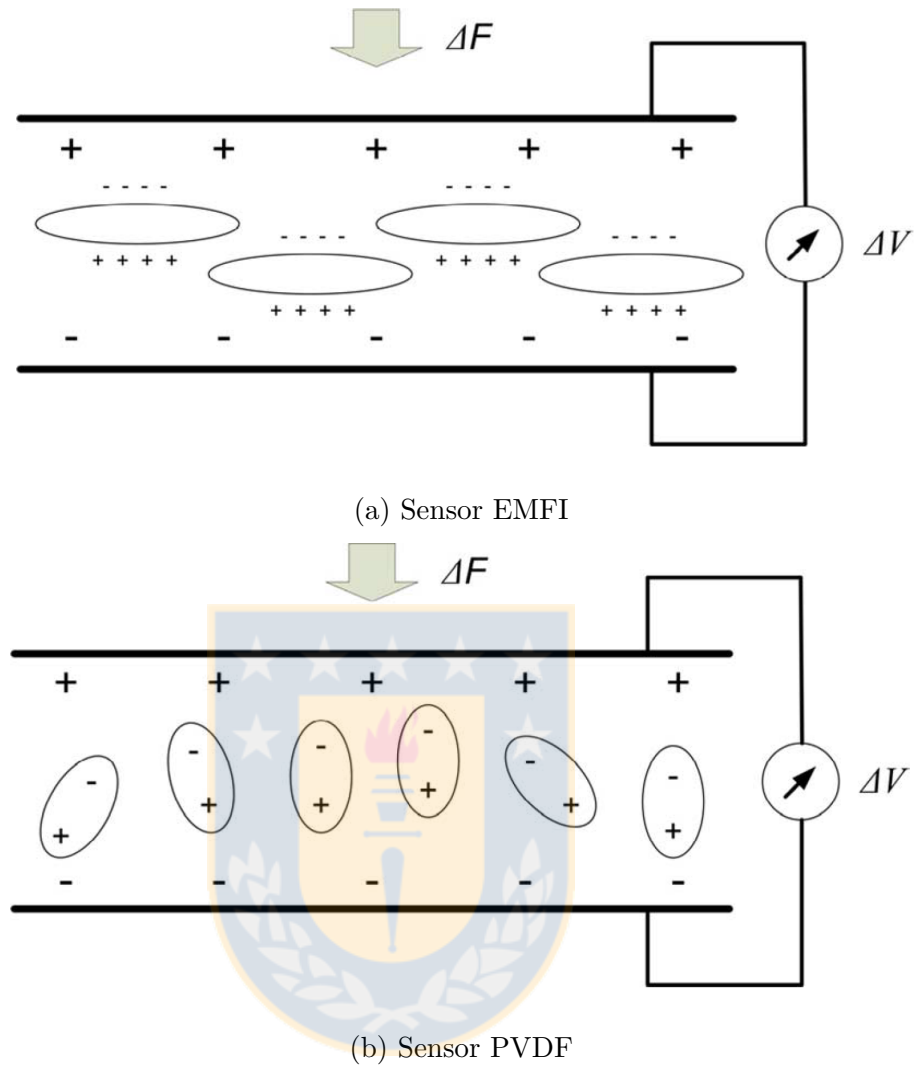


Figure 3.1: Simplified model structure of EMFi (a) and PVDF (b) sensors [11].

sensitivity approximately five times greater than the PVDF [12]. This characteristic gives a clue of what sensor should be used to measure cardiac activity and respiration movements.

Both sensors have enough sensitivity and precision to measure cardiac and respiratory activity [6]. Cardiac activity is related to the action-reaction force of the body, caused by the heart when it pumps blood through the aorta. This acquired signal is called ballistocardiogram (BCG), which is a graphic representation of this

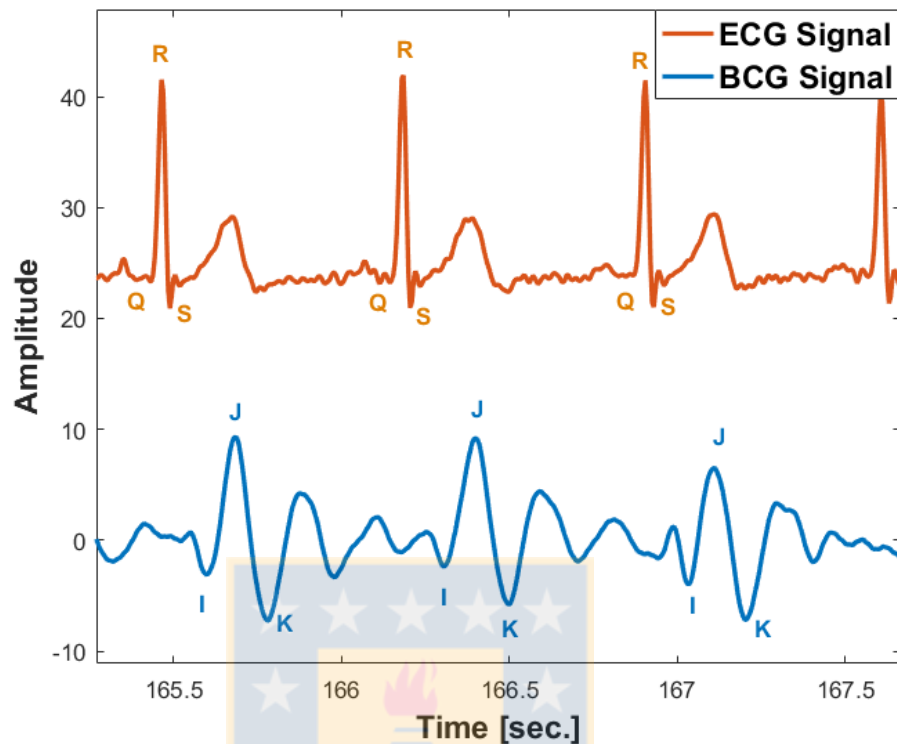


Figure 3.2: Electrocardiogram and Ballistocardiogram signals.

action-reaction force (Fig. 3.2). The most characteristic waveform of BCG is the IJK wave, which occurs when the blood is ejected from the left ventricle. This is a mechanical signal, and it has a phase shift with the electrocardiogram (ECG).

Breathing activity involves a series of movements of many muscles of the rib cage, such as the diaphragm, intercostal muscles, abdomen, etc. These movements are captured together with the BCG (Fig. 3.3).

Different types of current-voltage transducers as charge amplifier [13] or use the non-inverting voltage amplifier [11] is suggested for the acquisition of the signals coming from sensors, so that it can be digitized by a digital-analog converter.

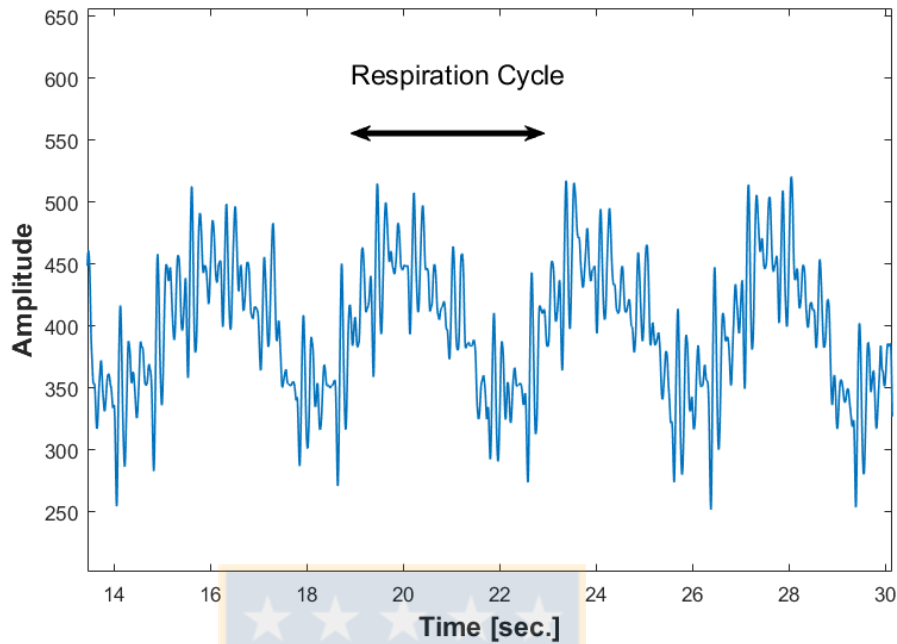


Figure 3.3: BCG signal with respiration baseline.

### 3.1.2 Signal Preprocessing

The preprocessing of the captured signals is important because sensors can acquire overlapping respiration and BCG signals. They must be separated in order to analyse them independently. Different ways to separate signals have been implemented. One technique is using analog or digital filters, taking advantage of the fact that the signals have different spectral band frequencies. Respiration signal has a frequency band between 0.1 and 0.5 Hz, and the BCG, between 1 and 20 Hz [11].

Statistic methods also are used to separate signals, such as independent component analysis. This method decomposes a signal into statistically independent components (ICA) [14]. Other methods are based on linear algebra to form orthonormal components and thus are linearly independent. This method is called principal component analysis (PCA) [15].

One of the most widely used methods for separating signals is the wavelet trans-

form [16–19], which has had many applications in the field of biomedical signals [20]. The wavelet transform consists on decomposing signals into different levels of details using a special filter banks. By choosing the proper details levels, the BCG and respiration can be rebuilt separately, using a reconstruction algorithm. Another popular method is the empirical mode decomposition (EMD) [21]. It uses a recursive algorithm that computes the upper and lower envelope of the signal, and then, subtract the mean of those signals from the original signal to obtain the intrinsic mode function. Next, a residual signal is obtained, subtracting the current signal with the function obtained. Later, with the residual signal, the algorithm is again applied, and so on.

Once the signals are separated, different algorithms can be used to analyse them independently.

## 3.2 Algorithms

### 3.2.1 Heartbeats Detection

Different algorithms have been developed in order to detect hearts beats from the BCG and calculate the heart rate. Some algorithms work with the raw signal, like using peak detector to find the J wave of the heart beats [22]. Other works extract the main characteristic of BCG beats in a training phase, obtaining a pattern and then comparing this pattern with the characteristics of the following BCG beats [23]. Another work focuses on the shape of the BCG beat, assuming that the beats have an “M” shape, and using a clustering method to discard the noise from the BCG beats [24]. Another approach is to calculate the similarity of the beats with a template beat, using correlation. The peak values of correlation are considered beats [25].

Other works focus on applying different transformations on the signal in order to facilitate the beat detection. Some works calculate the energy of the signal and use

a peak detector to find the maximum points of energy [8] [26]. The length transform has also been applied, based on the assumption that the largest part of the BCG beat is the IJK wave, and then apply a local peak detector [27] [28]. Other work proposes to use a sliding window and obtain the fast Fourier transform to obtain the spectral power, which indicates the periodicity of the signal [29].

### 3.2.2 Respiratory Cycles Detection

Respiration signal is easier to analyse compared with the BCG signal. It has a lower frequency content, and the signal is similar to a pure harmonic.

Some studies are focused on detecting respiration cycles using a filtered respiration signal, in order to detect semi-cycles (inspiration and expiration). A semi-automatic algorithm uses a moving mean window to filter the respiration signal. First, the waveform is separated into breath cycles by identifying intercepts of a moving average curve with the respiration signal. Peaks and valleys were then defined as the maximum and minimum respectively. Finally, automatic corrections and manual user interventions were employed [30]. A noise-robust respiratory cycle detection algorithm is proposed, with the same principle of filtering the respiration signal in order to detect breath cycles. The analysis is made under the assumption is that only breaths of 'typical sizes' are real respiratory efforts, and the deviation from a typical-size breath leads to poor data quality. The algorithm identifies typical breaths by dynamically adjusting its breath identification criteria, based on the initially identified breaths [31]. The width, area and height of the breath cycle are calculated in order to determine if it is noise or a real breath.

Unlike to two algorithms previously mentioned, other work detect breath cycles using 2 points (P1 and P2) of the signal. Those points have a distance of N samples. In every iteration the points are moved in 1 sample. If the difference between P2 and P1 is positive and in the next iteration the difference is negative, the algorithm find the max value between the points. If the difference in negative and in the next



iteration is positive, the algorithm find the minimum value. Then, the amplitude of breath cycle is calculated using the maximum and minimum values obtained. If the amplitude is greater than a fixed threshold, it is considered as a valid respiration. Otherwise it is considered noise.

### 3.2.3 Noise Detection

The use of pressure sensors allows the extraction of physiological signals in a non-invasive way. However, the disadvantage is that they are sensitive to motion artifact, like moving the arms or legs, or even talking. That disrupt BCG and respiration signal, causing the algorithm to fail in estimating the HR and RR properly. It is necessary to have an algorithm capable of detecting unwanted noise, in order to avoid false estimation. Also, the disadvantage of a non-obtrusive pressure sensor is the force distribution sensitivity. Research show that even the different position of the subjects over the sensors have an effect on the amplitude and quality of the signal [32] [33].

Several works detect noise artifact using a high order statistic indexes like standard deviation (SD) or kurtosis [28] [34] [35]. Other works use an auxiliary sensor to detect vibration [8], like an accelerometer. In order to stablish if the subject was in motion, the RMS value is calculated, and compared to a fixed threshold [35].

Other work proposed the use of a vibration sensor, which detects vibrations in the ground and it is used as a reference, in order to make a noise cancellation techniques [36].

## 3.3 Alarms Criteria

For the detection of cardiac abnormalities, 2 methods have been developed. One method analyses the evolution of the instantaneous heart rate [37], and the second one analyses the mean heart rate by epochs [38] [39]. Those criteria are also applicable to the respiratory signal.

A HR is considered normal when its value is between 60 and 100 beats per minute. Bradycardia is reported when the HR is less than 60 beats per minute and tachycardia, when the HR is greater than 100 beats per minute [40]. On the other hand, when there are no QRS complexes for more than 4 seconds, it is considered asystole [38].

For respiratory activity, a normal RR is considered when it is between 12 and 20 breaths per minute. Bradypnea is considered when RR is below 12 breaths per minute and tachypnea when RR is above 20 breaths per minute [41].

### 3.4 Discussion

The development of non-invasive systems for the measurement of respiratory and cardiac activity is oriented to the patient, so that the system is comfortable and simple to use, thus avoiding the supervision of a specialist when in use. Therefore, pressure sensors meet with the non-invasive definition, and make them the best option to develop a measurement system.

However, depending on the application, the correct sensor must be chosen. For example, the EMFi and PVDF are sensitive to the vibrations generated by the heart pulse, so they can be used to capture cardiac and respiration activity. But, for the same reason, they are sensitive to body movements, which distort those signals. In addition, they do not detect static forces, so there is no way to know if a subject is positioned over the sensor. On the other hand, resistive sensors are able to detect static forces but do not have enough sensitivity to detect cardiac activity. One solution would be to integrate sensors to detect both kind of forces and have better information on the patient's condition, although the system is more complex when more sensors are included.

Regarding the pre-processing of signals, all separation methods have delay associated depending on their complexity. This issue is important to consider in order to implement algorithms in real time. The use of analog or digital filters is the simplest

alternative. The use of analog filters avoids extra digital processing but increases the hardware size. Digital filters are another option. Infinite Impulse Response (IIR) filter type is an option to process the signal with a low numbers of coefficients (low processing).

The wavelet transform is a useful method to separate signals, but it takes more processing to obtain the different levels of details, in order to rebuild signals of interest. Also, the quality of the rebuilt signal depends on the filter bank order used. Lower orders of the filter causes worst reconstructions of the details, and greater order of the filter make a better rebuilds, but longer processing time will be needed.

The correlation method is a viable alternative for the detection of beats, but a reference BCG heartbeat is required for each particular person. Applying transformations to BCG signal makes it less complex and easier to analyse.

For RR estimation, the size of the window to analyse the signal is fundamental. Respiratory signal varies its duration depending on if there are fast or slow breaths. It is necessary to consider a suitable window size to be able to detect all ranges of the respiratory rates.

Proposed noise detection methods have a disadvantage. They consider a noisy signal when its amplitude or its variability increases caused by body movements. But, bad quality signal does not imply a body movement that distorts the signal. It could also be caused by the limitation of sensors to capture force distribution, which alters the accuracy of the algorithms previously described. In this case, a better noise detection algorithms would be needed, independent of the amplitude of the signal.

The instantaneous HR analysis offers better monitoring of HR evolution. However, in case of any false negative or false positive, it produces a false datum. For epoch analysis, an average of the instantaneous frequencies is calculated, filtering the extreme values, making it more robust to false alarms, but this implies an associated delay when the alarm is triggered.

# Chapter 4

## System Description

In this chapter the complete system is described at each stage, and how the system is energized.

### 4.1 System Stages

The acquisition system was set on a chair with cushions for the comfort of the subjects. The system captures the data from the sensors while the subject is sitting. The acquisition system is divided into 5 stages: 1) Unobtrusive sensors, 2) Analog circuit, 3) Analog to Digital conversion (ADC), 4) Single Board Computer (SBC) and 5) Wireless communication. An overview of the implemented system is presented in Fig. 4.1.

#### 4.1.1 Unobtrusive sensors

The system uses 3 types of sensors: an Electromechanical Film (EMFi), Polyvinylidene Difluoride (PVDF) and Force Sensing Resistors (FSR).

One EMFi L-Series of 30x29 cm sensors was used and placed on the seat of the chair. This sensor is responsible for measuring cardiac activity. Two PVDF of

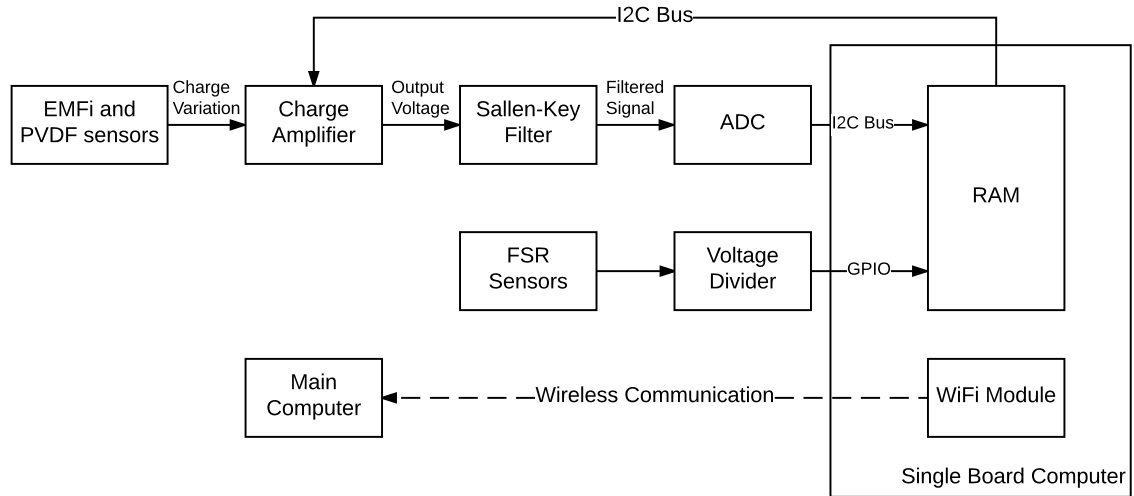


Figure 4.1: General System Diagram.

152mmx76mmx0.06mm are set on the backrest. They are responsible for measuring respiration activity. Finally, 2 FSR are set on the chair, one on the seat, and one on the backrest. They are responsible for detecting presence of the subject and trigger the calibration stage and the respiration and cardiac signals algorithms (Fig. 4.2).

#### 4.1.2 Analog Circuit

The analog circuit was first implemented on a protoboard. Then, for the final design it was printed on a circuit board, designed with EAGLE CadSoft software. A charge amplifier is used to amplify the charge variation from the EMFi and transduce it to a variation of voltage. The circuit also has a digital potentiometer, configurable using the I2C communication protocol, allowing 256 steps of resistance. This resistance value is configured during the calibration stage in order to set the gain of the circuit. The same charge amplifier is used for the PVDF sensors, but its gain resistance is fixed (Fig. 4.3).

The amplified signal from EMFi is filtered using a second order low pass Sallen-

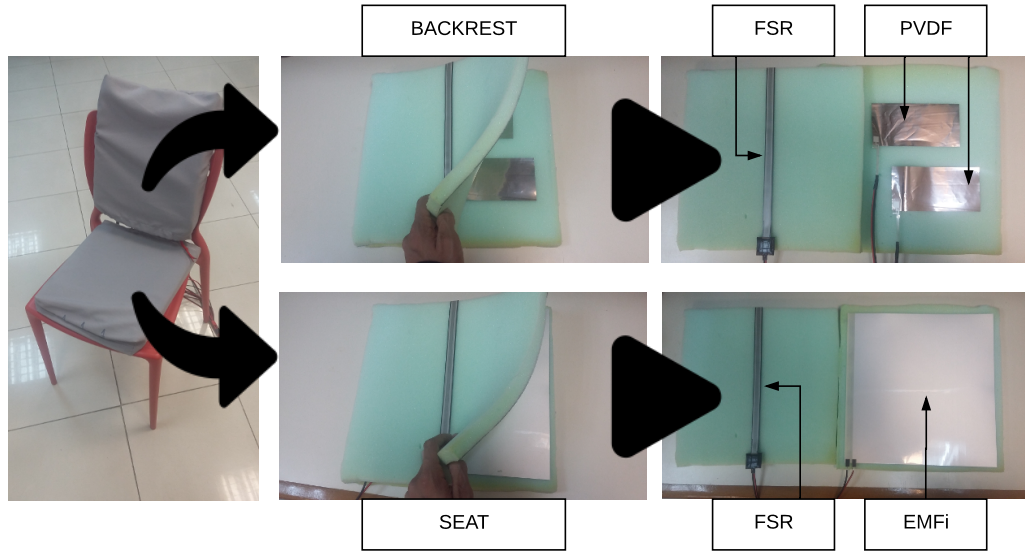


Figure 4.2: Sensors on a chair. Sensors setted on a common chair. EMFi is placed on the seat to capture BCG and 2 PVDF sensor are placed on the backrest to capture respiration. FSR sensors are placed on seat and backrest in order to detect the presence of subjects.

Key filter with 20 Hz cutoff frequency. The 2 signals coming from the PVDF sensors are filtered using the same type of analog filter, but the cutoff frequency is 0.5 Hz. Finally, these three signals are acquired through the analog-digital converter.

For the FSR, the system uses a voltage divisor and both outputs are connected directly to two digital inputs of the SBC (Fig. 4.4). When a subject is setting over the sensor, the output voltage is near to 3.3V, representing a high logic voltage and when there is no forces applied on the sensor, the output voltage is near to 0V, representing a low logic voltage.

### 4.1.3 Analog to Digital Conversion (ADC)

An Analog-Digital Converter ADS7828 is used for digitalizing the signals coming from the EMFi and PVDFs sensors. It has 12 bits of resolution, and communicates

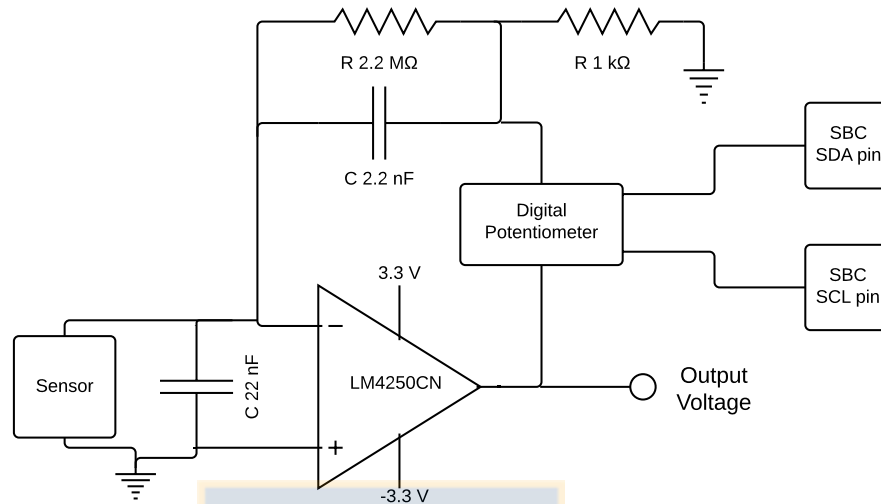


Figure 4.3: Charge Amplifier. This circuit transduces the variation of charge of sensor into variation of voltage. A digital potentiometer is used to adjust the gain for EMFi, for PVDF a fixed resistance is used.

with the SBC using I2C protocol to send the acquired signals at 100 S/s.

#### 4.1.4 Single Board Computer (SBC)

The SBC is a useful alternative to a micro-controller for embedded applications as a micro-controller, and have enough resources to make complex processing as a modern computer. A Raspberry Pi 3 was used to implement the system (Fig. 4.5). Table 4.1 shows the characteristic of the SBC.

Python language and the MRAA library are used to implement the I/O control. Through the I2C bus pins, the software controls the ADC, the digital potentiometer and the digital input from the FSR circuit. The digital inputs are read at 100 S/s.

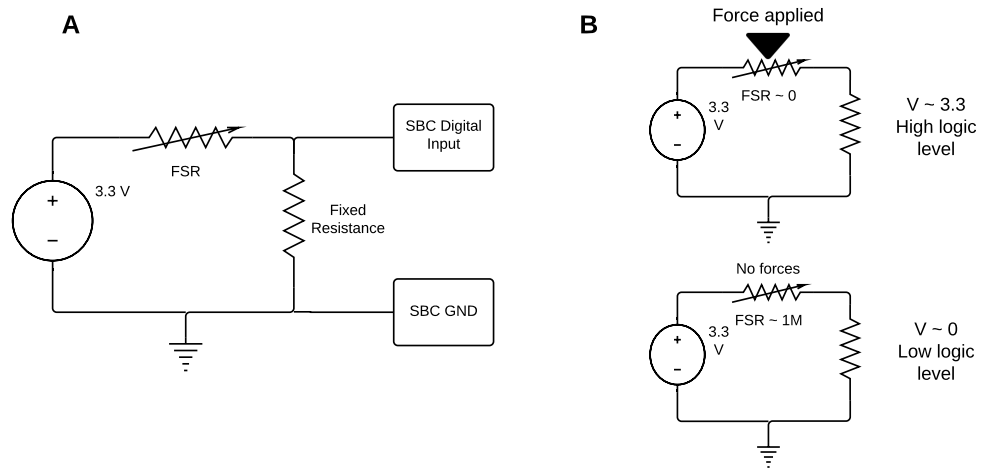


Figure 4.4: FSR circuit. **A:** Voltage divider circuit **B:** When a force is applied to the FSR, its resistance becomes low, and the output voltage is a high level logic. On the other hand, if there is no forces applied on it, the output voltage is a low level logic.

#### 4.1.5 Wireless Communications

The Raspberry Pi send the diagnosis of respiratory and cardiac activity using the WiFi module. A TCP/IP communication was implemented using the Socket library from Python.

Table 4.1: Raspberry Pi 3 Features

CPU	ARM Cortex-A53 Quad Core Processor SoC running @ 1.2GHz
RAM	1 GB RAM
USB	4 USB 2.0
Storage	microSD
Network	BCM43143 WiFi, 10/100 Ethernet (RJ45)
Low-Level Peripherals	27 x GPIO, UART, I2C bus, SPI bus, +3.3V, +5V, Ground
Power Requirements	5V @ 2.4 A via microUSB power source
Operative System Supported	Raspbian, Windows 10 IoT Core
Dimensions	85mm x 56mm x 17mm



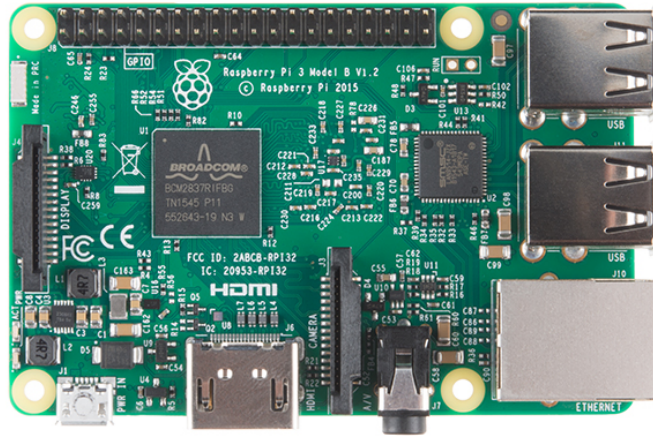


Figure 4.5: Raspberry Pi 3.

## 4.2 Power Supply

The Raspberry Pi 3 is powered with a  $\mu$  USB charger of 5V, with a maximum current of 2 Amps. It has a 3.3 V output peripheral, used for powering the analog circuit and the ADC. The analog circuit has a dual supply operational amplifiers, and the negative voltage supply (-3.3 V) is given by a charge pump circuit ADM8660, that inverts the positive voltage.

The analog system and the ADC in idle mode, i.e. without a person on the chair and without acquiring data, needs a current of 3 mA. With a person on the chair and acquiring data, the systems needs 6 mA. The maximum permitted current draw from the 3.3 V Raspberry pin is 16 mA, therefore the system meets these requirements.

The current needed for Raspberry Pi in order to run the algorithms is analysed in the Results chapter.

# Chapter 5

## Algorithms and Signal Processing

This chapter describes the calibration stage, the BCG and respiration signal processing and their diagnosis. These algorithms were implemented in Python.

### 5.1 Calibration Stage

This processing is necessary to calculate the variability thresholds and amplitudes for the analysis of the respiratory signal ( $r1$  and  $r2$ ), and to define a minimum gain and a threshold of minimum variability for the BCG signal. Both FSR sensors must be active to start the calibration.

The algorithm set 10 different gains (steps of resistance), sorted from lowest to highest. When the calibration starts, the lowest gain is configured in the digital potentiometer. Every 5 seconds, the last 500 acquired samples of each signals is analysed. The standard deviation of the BCG signal is calculated. If it is less than 200, the next value of gain is configured in the digital potentiometer, if it is between 200 and 300, the gain is kept constant, and if it is greater than 300, it is considered noise. For the respiratory signal, the range and the standard deviation is calculated every 5 seconds. When there is noise in the BCG signal, respiration signal is also considered as noise.

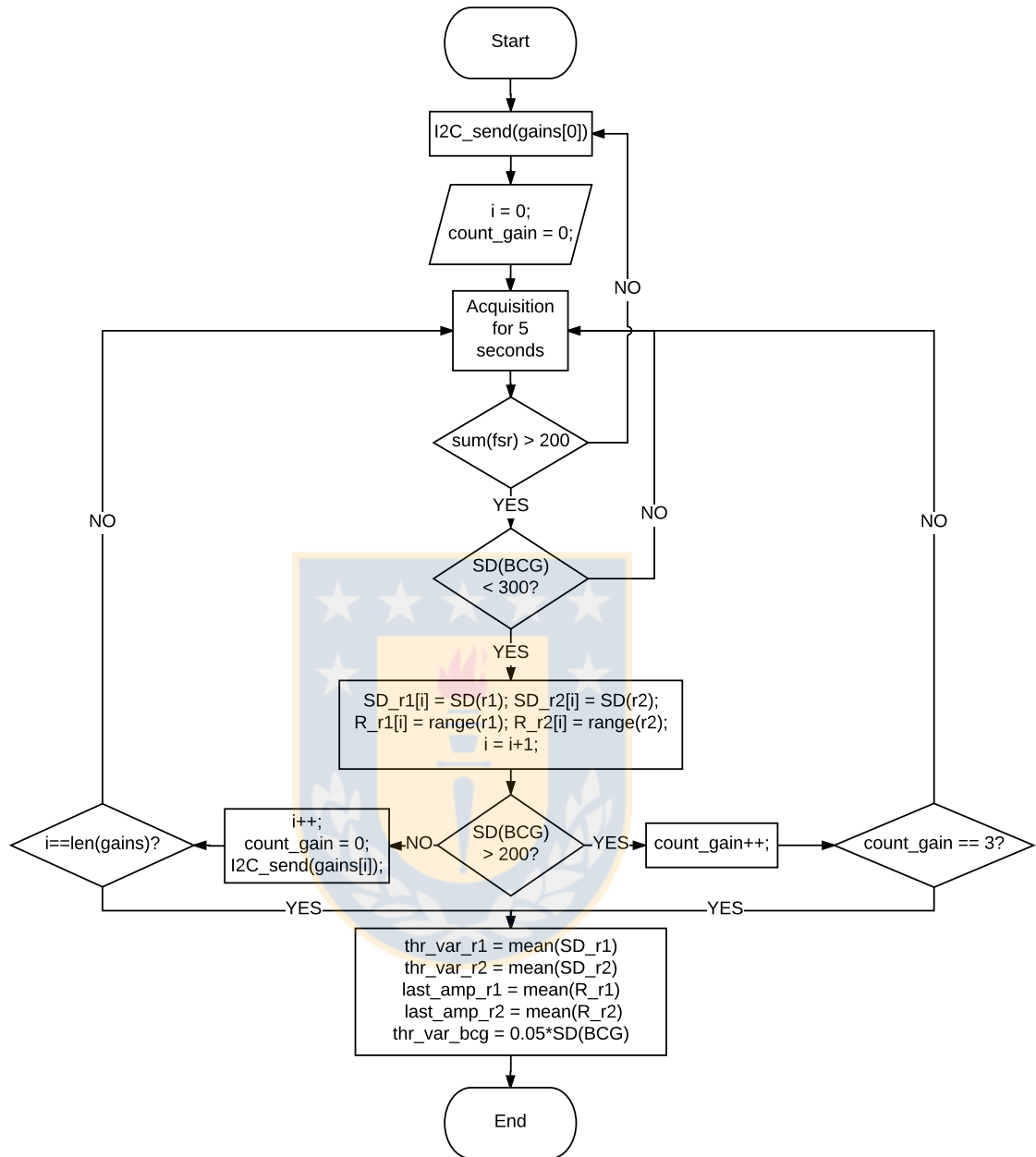


Figure 5.1: Calibration Flow Chart.

When the gain is maintained for 3 consecutive iterations, the calibration is completed, and thresholds are calculated (Fig. 5.1).

## 5.2 BCG signal processing

The algorithm analyses segments of 15 seconds of BCG, with an overlap of 10 seconds. A band-pass 2-20 Hz butterworth digital filter was used to filter the incoming BCG signal.

### 5.2.1 Peak Detection

The algorithm for estimating the HR was already described in [42] [28]. It includes the following steps:

- Signal separation: Wavelet Transform was used to separate the BCG signal from Respiration signal. Using the mother wavelet 'Deabuchie 6', the raw signal was separated. Then, using details 4 to 7 the clean BCG signal was rebuilt.
- Length Transform: Since IJK wave is the largest wave, the length transform (LT) is calculated using a moving window of 60 samples. Then the LT is smoothed (SLT) using a moving average filter of 60 samples.
- Peak detection: Peaks are detected finding local maxima in a neighbourhood of  $\pm 30$  samples in the SLT signal.

Wavelet transform offers good signal decomposition without phase or amplitude distortion, but it requires complex computing to obtain details and approximation coefficients to rebuild the filtered BCG signal. In order to make a fast signal processing, wavelet transform was replaced using a 5th order band pass 2-20 Hz digital IIR filter.

Calculating the LT (Eq. 5.1) is computationally expensive, so an approximation was performed (Eq. 5.2). Finally, the SLT is calculated (Eq. 5.3), with L as the window size.

$$LT[k] = \sum_{i=k-L}^k \sqrt{(S[i] - S[i-1])^2 + 1} \quad (5.1)$$

$$LT[k] = \sum_{i=k-L}^k |S[i] - S[i-1]| \quad (5.2)$$

$$SLT[k] = \frac{1}{L} \sum_{i=k-L}^k LT[i] \quad (5.3)$$

Usually, the window length to find the peaks is fixed, meaning that it would have problems calculating higher or lower frequencies than a ‘normal’ HR. At high frequencies, the windows would include more than one beat. At low frequencies, the windows can show a BCG rebound signal as a beat.

The solution to this problem is the proposed adaptive length neighborhood based on the variability of multiple SLT.

### Multiple Smoothed Length Transform

To avoid having one fixed window size, we propose to use multiple STL of the BCG signal, using 4 fixed size windows of 80 ( $SLT_{80}$ ), 40 ( $SLT_{40}$ ), 20 ( $SLT_{20}$ ) and 10 ( $SLT_{10}$ ) samples in order to determine the best neighborhood length for peak detection (Fig. 5.2). Also, another STL of 5 samples ( $SLT_5$ ) was calculated for the peak detection. Then, a phase shift correction is applied to the SLT to realign with the original signal.

Larger windows avoid detecting false beats from bounces, but do not respond well to high frequencies, because the heart beat period is smaller than half of window size. On the other hand, smaller windows detect heart beats at a high frequency, however, they are sensitive to rebound and detect false positives at low frequencies.

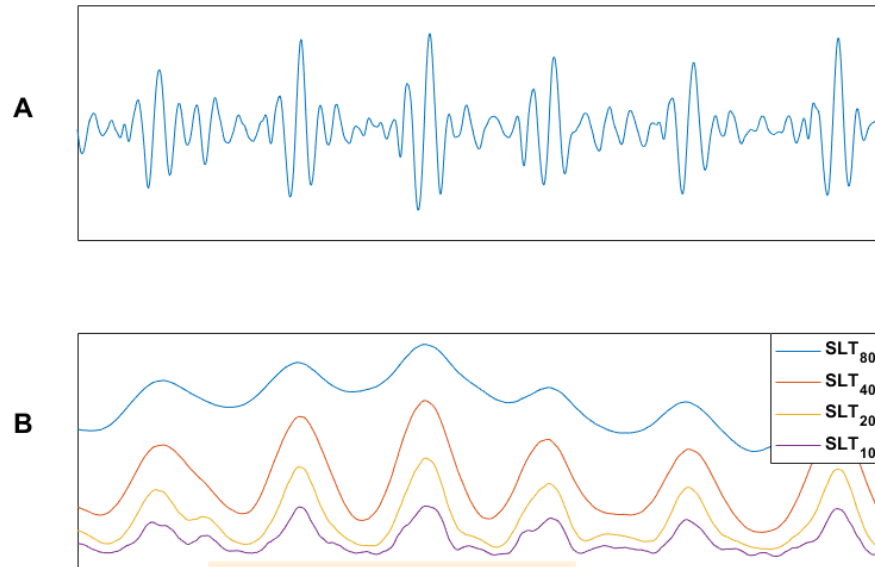


Figure 5.2: Multiple Smoothed Length Transform. **A:** BCG signal, **B:** Multiple Smoothed Length Transform.

### Neighbourhood's Length estimation and peak detection

Neighbourhood's Length (NL) depends on the parameter  $L$ , which varies depending on the variability of the last  $N$  samples of the SLT signals, and a constant  $f$  (Eq. 5.4). These variabilities are ordered from highest to lowest. If  $VAR_{STL_{80}} \geq VAR_{STL_{40}} \geq VAR_{STL_{20}} \geq VAR_{STL_{10}}$ ,  $L$  will be equal to 80. Else if  $VAR_{STL_{40}} \geq VAR_{STL_{20}} \geq VAR_{STL_{10}}$ ,  $L$  will be equal to 40. Else if  $VAR_{STL_{20}} \geq VAR_{STL_{10}}$ ,  $L$  will be equal to 20. Otherwise,  $L$  will be equal to 10.  $N$  and  $f$  are experimental values that in the algorithm performs best for  $N = 50$  and  $f = 0.5$ .

$$LN = 2 \cdot L \cdot (1 + f) \quad (5.4)$$

When the peak detection algorithm starts on the SLT5, the NL is estimated point by point and if the actual point value, located in "i", is the maximum value on a

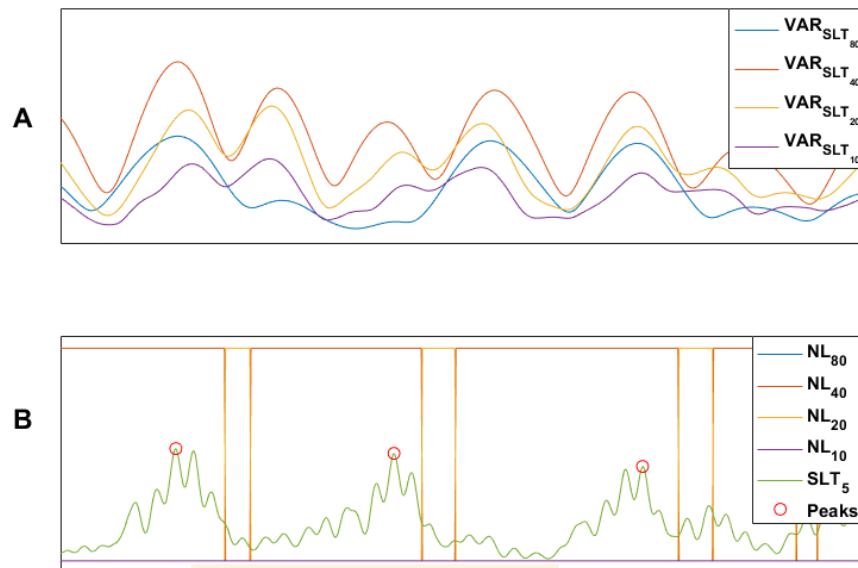


Figure 5.3: Neighbourhood Length Estimation. **A:** Variance of SLT, **B:** Peak detection using Neighbourhood Length estimated.

neighborhood of  $i - NL = 2$  :  $i + NL = 2$ , a peak is detected. (Fig. 5.3)

### 5.2.2 Noise Estimation

One of the main problems of unobtrusive measurement is noise. Noise has different sources, for example, muscle movements, breathing, talking or even walk near the sensors. To differentiate noise signal from clean BCG, the signal quality is assessed. A new approach was developed in this work to detect noisy BCG segments using correlation [43] and HR variability.

The correlation criteria is based on the assumption is that two clean beats are similar, hence with a high correlation (Fig. 5.4), but if there is a poor signal quality or if there is a false peak detected, the correlation between two extracted segments would be low (Fig. 5.5).

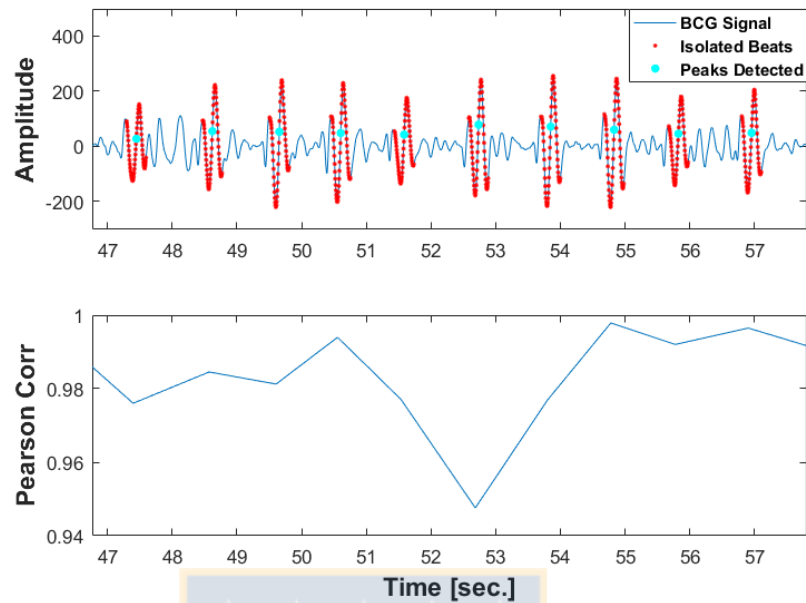


Figure 5.4: Good Quality Signal. Good quality if BCG. The correlation between beats is high.

The variability of the HR is an indicator of regular or irregular heart rate. Previous works mention different methods to estimate the heart rate variability using frequency domain techniques [44] [45], time domain techniques [46] and geometrical methods like Poincaré Plot [47]. In this work, time-domain techniques were used, calculating the standard deviation of 5 consecutive periods. Physiologically speaking, the HR has a normal variability that is constrained. When this variability is exceeded, the analyzed segment is considered noisy. Estimated HR variability indicates if there is a problem with the signal quality or if there is a problem with the algorithm (Fig. 5.7).

### Correlation threshold

From the detected peaks, the beats are extracted using a neighborhood of  $pm$  15 samples. Pearson's correlation coefficient between 2 consecutive beats is calculated



(Fig. 3). If the correlation between beats is low than a fixed value, the period between beats is discarded, otherwise is considered for HR and HRV calculations.

### HR variability thresholds

A fixed variability threshold ( $V_{Thr}$ ) of 0.25 s was selected to analyze the SD of 5 consecutive periods. If the SD value is over  $V_{Thr}$ , periods are considered noisy, otherwise the periods are considered reliable. This  $V_{Thr}$  is selected empirically from the MIT-BIH Normal Sinus Rhythm (NSR) [48] and the MIT-BIH Atrial Fibrillation (AF) [49] databases from Physionet (Fig. 5.6).

### 5.2.3 BCG Diagnosis Algorithm

A decision-tree algorithm was developed for the diagnosis. The tree is divided into 5 main components: 1) Presence detection, 2) Variability of BCG, 3) Peak

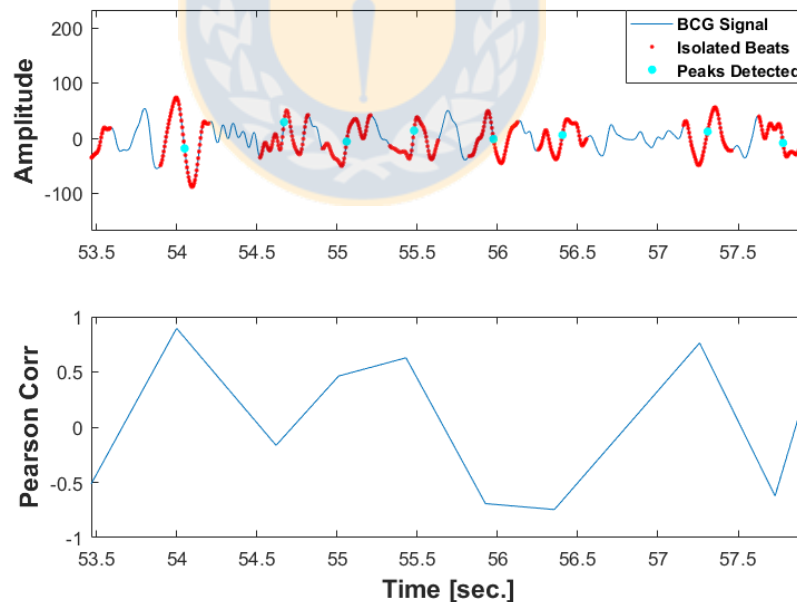


Figure 5.5: Bad Quality Signal. Bad quality of BCG. The correlation between beats is low

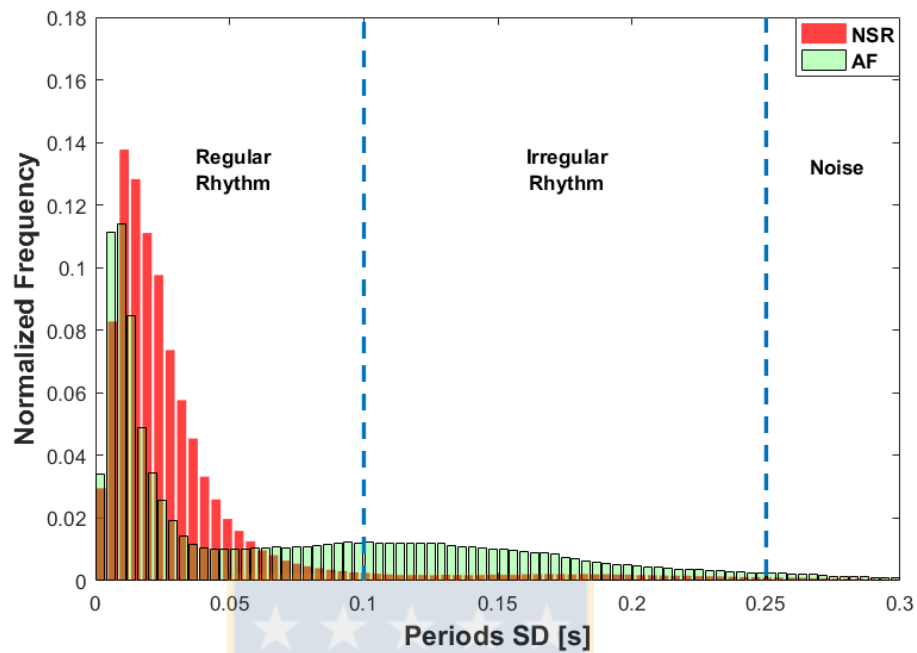


Figure 5.6: Histogram of periods SD in case of normal rate and atrial fibrillation. A fixed threshold of 0.1 s is selected to discriminate the regular from the irregular periods. A SD over 0.25 s is used for noise detection.

detection and Correlation filter, 4) Variability of periods and 5) Report (Fig. 5.8). The algorithm analyzes BCG segments of 15 seconds, with an overlap of 10 seconds. When the algorithm ends, it waits for the next segment of 15 seconds.

### Presence detection

The FSR sensor placed on the seat is used to detect when a person is sitting on the chair. If over 80% of the segment time the level is high, the algorithm assumes a presence and goes to the next node. Otherwise, the algorithm waits for the next segment.

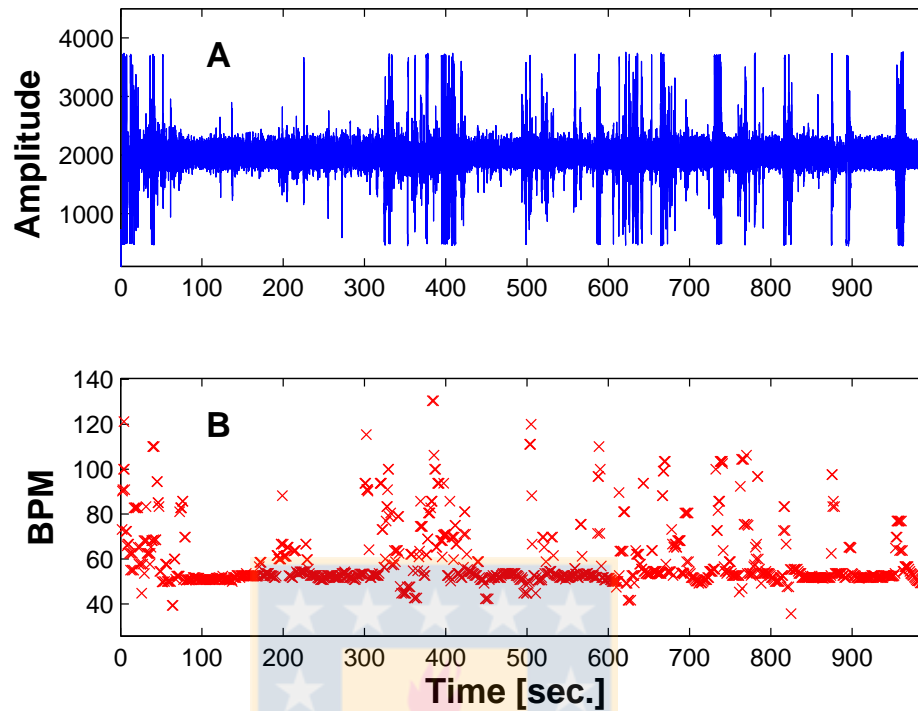


Figure 5.7: Heart Rate Variability by Motion Artifact. **A:** Raw BCG signal, **B:** Calculated HR. When a motion artifact occurs, the heart rate variability increases due to false detection of beats.

### Variability of BCG

A low variability of the signal is also important to analyse, because it indicates that the cardiac output is decreasing or the heart is in asystole. If the variability of the last 3 seconds of BCG segment lower than 0.2 times the variability threshold obtained during calibration ( $SD_C$ ), an asystole is reported. Otherwise, the algorithm continues to the next node.

### Peak detection and Correlation filter

The algorithm detects every possible beat using the adaptive neighborhood for peak detection. A fixed threshold of 0.9 is used to filter the correlations. If a peak

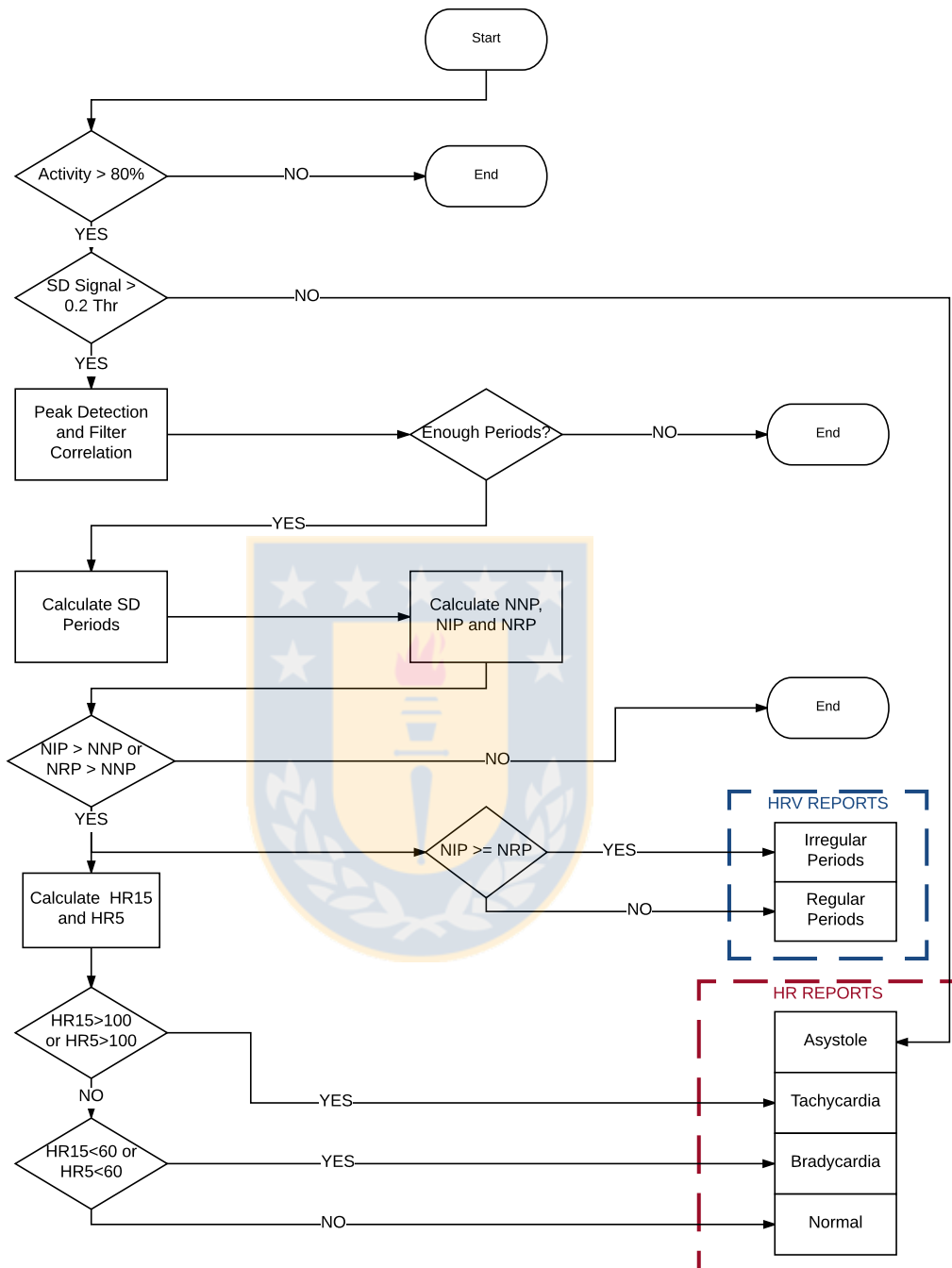


Figure 5.8: Flow Chart BCG Diagnosis Algorithm.

candidate has a correlation value lower than 0.9 with its predecessor, the beat periods delimited by those peaks is discarded. If there are less than 5 periods left, the algorithm does not continue the analysis because there is not enough information for the diagnosis.

### Periods Variability

Using a moving window of five samples, we calculate the standard deviation of the surviving periods. Then, two fixed thresholds are used in order to classify the variability of each segment in normal rhythm, irregular rhythm or noise. The variability must be lower than 0.1 to be classified as normal rhythm, between 0.1 and 0.25 to be classified as irregular rhythm, and higher than 0.25 to be classified as noise. If the number of noisy periods (NNP) is greater than the number of regular periods (NRP) or number of irregular periods (NIP), the segment is considered as noise and the analysis is stopped.

### Report

The algorithm reports an irregular rhythm if NIP is greater than NRP, otherwise the algorithm reports a regular rhythm. On the other hand, the algorithm calculates the mean heart rate of the entire segment of 15 s ( $\overline{HR}_{15}$ ), and calculates the mean heart rate of the last 5 s ( $\overline{HR}_5$ ) in order to report HR alarms. If ( $\overline{HR}_{15}$ ) or ( $\overline{HR}_5$ ) is greater than 100 BPM the algorithm reports tachycardia. If ( $\overline{HR}_{15}$ ) or ( $\overline{HR}_5$ ) is lower than 60 BPM, the algorithm reports bradycardia. If both ( $\overline{HR}_{15}$ ) and ( $\overline{HR}_5$ ) are between 60 and 100 BPM, the algorithm reports a normal HR condition. Asystole is reported according to BCG variability, as previously explained. Table 5.1 describes the different diagnoses and the conditions that trigger them.

Table 5.1: Different Reports on Diagnoses Algorithm

		Conditions
Heart Rate	Tachycardia	$\overline{HR}_{15} > 100$ or $\overline{HR}_5 > 100$
	Bradycardia	$\overline{HR}_{15} < 60$ or $\overline{HR}_5 < 60$
	Normal	$60 < \overline{HR}_{15} < 100$ and $60 < \overline{HR}_5 < 100$
	Asystole	$SD(BCGSegment_{10}) < 0.2 * SD \text{ Calibration}$
Heart Rate Variability	Regular	majority variability periods $< 0.1$
	Irregular	$0.1 < \text{majority variability periods} < 0.25$

### 5.3 Respiration Signal Processing

The algorithm analyses segments of 30 seconds of respiration signal, with an overlap of 20 seconds. It was implemented in [8], based on [30] [31]. The noise estimation algorithm was developed in the present work.

#### 5.3.1 Respiration Cycle detection

It consists on recognizing each respiration cycle, detecting its positive semi-cycle (inspiration) and its negative semi-cycle (expiration). Then, a symmetry and amplitude criteria were applied to pair semi-cycles, in order to recognize a respiration cycle or discard it as noise. Using a mean moving window of 500 samples, the respiration signal (RS) is filtered, obtaining its baseline (B). With this baseline signal, both positive and negative semi-cycles are detected. Where the baseline is lower than the respiration signal, there are positive semi-cycles or inspirations. Where the baseline is higher than respiration signal, there are negative semi-cycles or expirations.

Every positive semi-cycle is continued by a negative semi-cycle, and their features are extracted: width (N), area (A) and amplitude (Fig. 5.9). The width is the number of samples of the semi-cycle (N). The area is calculated using eq. 5.5.

$$A = \sum_{i=k}^{k+N} |RS[i] - B[i]| \quad (5.5)$$

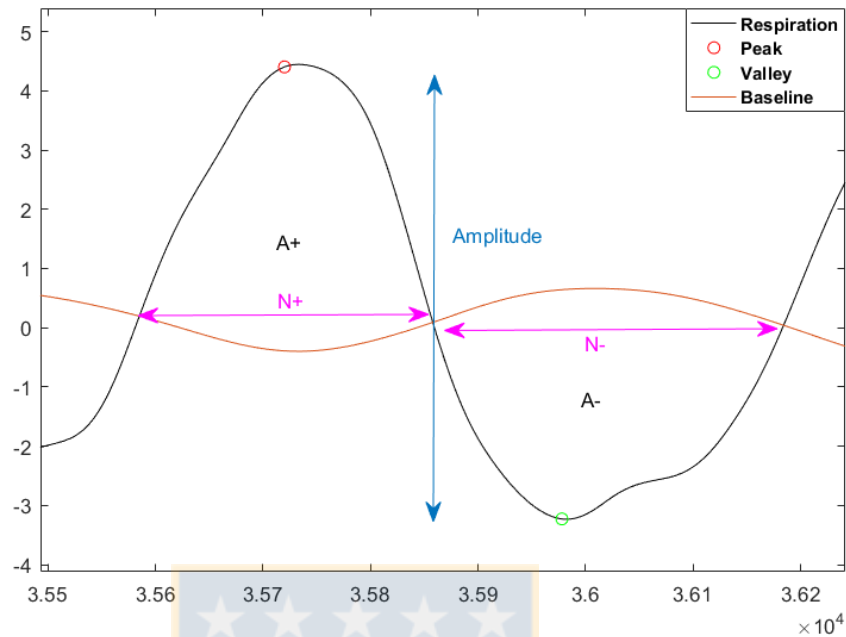


Figure 5.9: Respiration algorithm criteria.

The amplitude is the maximum value of the positive semi-cycle minus the minimum value of the negative semi-cycle. Then, a decision stage consists on three conditions:

- The ratio of  $N+$  to  $N-$  is greater than 0.3 and less than 1.3.
- The ratio of  $A+$  to  $A-$  is greater than 0.4 and less than 2.5.
- The absolute amplitude of the current respiratory cycle should be greater than 50% and lower than 200% the amplitude of the previous respiratory cycle.

### 5.3.2 Noise Signal Detection

The respiratory signal can be distorted by the subject activity, like body movements and talking. Kurtosis was chosen to measure the respiration signal quality (Fig. 5.10). When the kurtosis of the signal is lower than a fixed threshold of 2.7,

the signal is classified as clean signal. Otherwise, it is considered noise.

### 5.3.3 Respiration Diagnosis Algorithm

A decision-tree algorithm was developed for the diagnosis (Fig. 5.11).

#### Presence detection

The FSR sensor placed on backrest detects if the subject is supported on it. If during 80 % of the time segment the level was high, the algorithm will go to the next node, otherwise, the algorithm waits for the next segment.

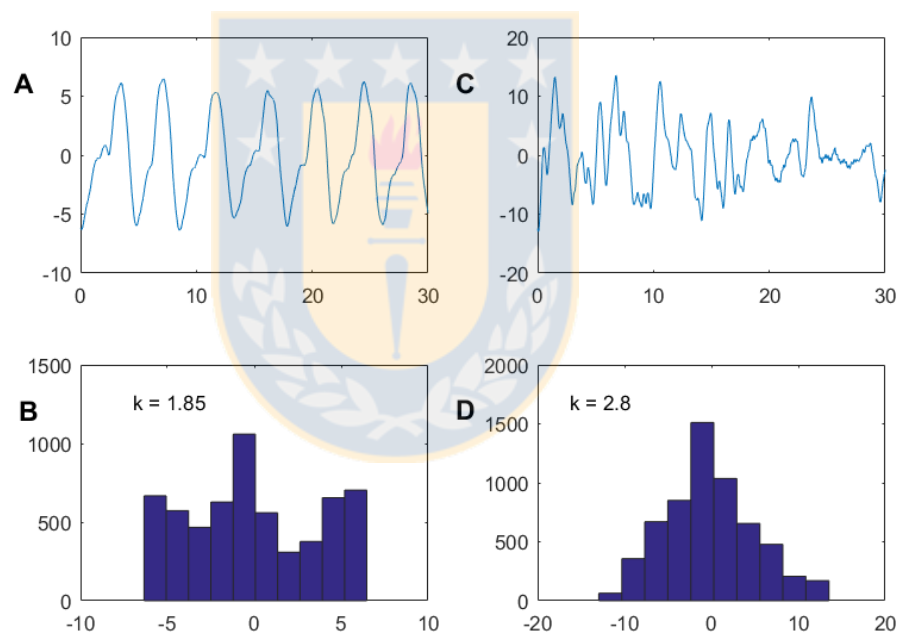


Figure 5.10: Respiration quality. **A:** High quality respiration signal, **B:** Histogram of high quality respiration signal, **C:** Poor quality respiration signal, **D:** Histogram of poor quality respiration signal.



### Choose the best respiration signal

There are 2 PVDF sensors capturing the respiration signal from the backrest. The respiration signal with a lower kurtosis is selected to extract the RR. Then, the

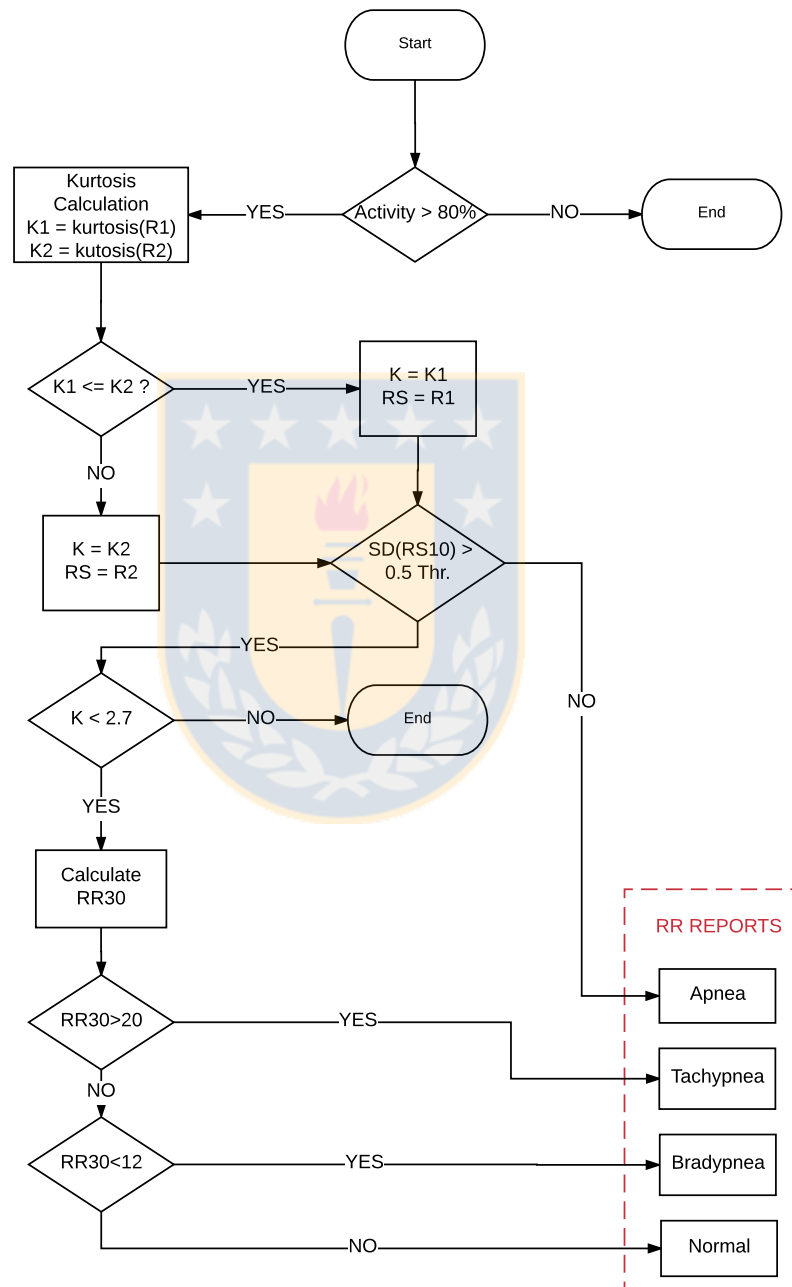


Figure 5.11: Flow Chart Respiration Diagnosis.

Table 5.2: Respiration Diagnosis

	Condition
Normal RR	$12 < \overline{RR} < 20$
Taquipnea	$\overline{RR} > 20$
Bradipnea	$\overline{RR} < 12$
Apnea	$SD(signal_{10}) < thr. Var$

algorithm goes to the next node.

### Respiration Signal's Variability

If there are no respiration cycles, the signal variability decreases. In order to detect when the respiration stops, a variability threshold calculated from calibration was implemented for detecting this event. If the SD of the last 10 seconds of the segment is lower than the fixed variability threshold, an apnea is reported. Otherwise the algorithm goes to the next node.

### Noise Detection

If the respiration signal has a kurtosis higher or equal to 2.7, the segment is classified as a noisy segment, and there is no report. Otherwise, cycle respirations are detected from the respiration signal.

### Reports

The algorithm calculates the mean RR of 30 second segment. If the RR is higher than 20, a taquipnea is reported. If the RR is lower than 12, a bradipnea is reported. If RR is between 12 and 20, a normal RR is reported. Table 5.2 describes different conditions for the diagnosis to be reported.

# Chapter 6

## Measurements and Simulations

This chapter describes the methodology for the measurements to validate the diagnosis algorithms, and the simulation performed.

### 6.1 Measurements

The measurements were divided into two groups: in a laboratory, with healthy subjects and in a hospital, with subjects with atrial fibrillation (AF). In both cases, the ECG , BCG signal and respiration signal were measured in parallel using a BIOPAC system acquisition, with a sampling frequency of 100 S/s. These were used to validate the diagnosis algorithm using as references peaks from the ECG [50]. Laboratory measurements were used to validate heart rate alarms and hospital measurements were used to validate irregular rhythms alarms. This test protocol was approved by the hospital's ethics and scientific committee of institutional review board (IRB).

#### 6.1.1 Laboratory Measurements

In the lab environment, 34 subjects were measured. Each measurement was divided into two parts:

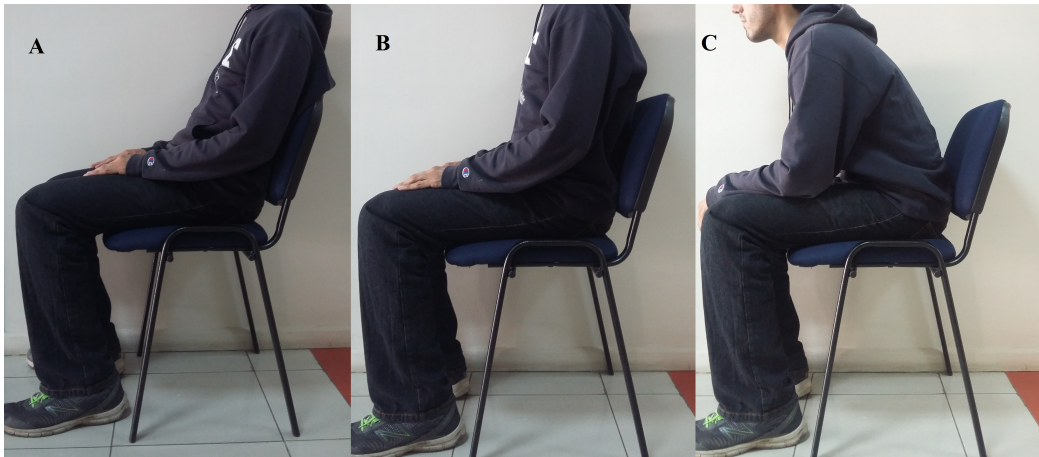


Figure 6.1: Different positions for measurements: A) Resting on backrest, B) Rest without the backrest and C) Resting on thighs.

1. Resting state: the subject was measured in 3 different positions on the chair:
  - 1) Leaning on backrest, 2) Sitting without backrest support and 3) Resting on thighs (Fig. 6.1). For each position they were asked to perform the following sequence: 1) Stay quiet, 2) Talk (Read a text aloud), 3) Talk with gesticulation, 4) Move legs 5) Move head from side to side and up and down and 6) Write a message on a mobile phone. This sequence was designed to observe the quality of BCG and respiration signals during different activities while seated. This sequence was repeated for each position.
  
2. After physical activity: the subject performed physical exercise for 1 minute. Then, the subject sits on the chair leaning back, and was measured during 3 minutes. After that, the subjects were asked to stop breathing for 20 second to simulate apneas (Fig. 6.2). This was done 3 times, breathing normally between these events.

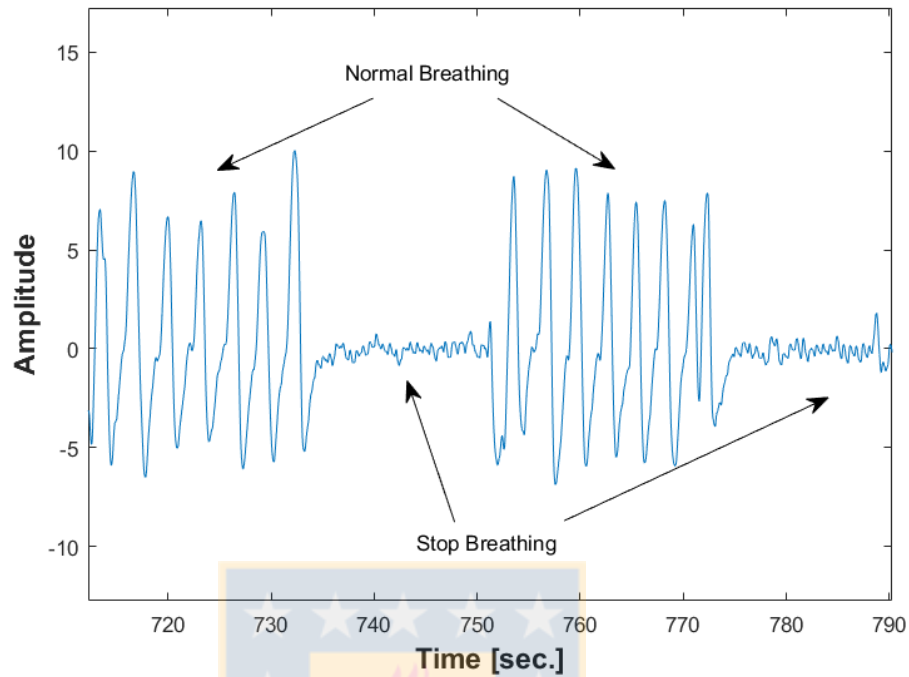


Figure 6.2: Apneas Simulation.

### 6.1.2 Hospital Measurements

24 subjects presenting atrial fibrillation (AF) were measured. All volunteers were informed about the study and asked to sign an informed consent. The patients were asked to remain as quiet as possible for 3 minutes. No patient showed discomfort when using the system.

## 6.2 Signals Simulations

In order to evaluate the diagnosis algorithm, this work considers the standard alarm criteria and delays described by ANSI/AAMI EC13: 2002 of cardiac monitors [51]. In order to simulate the cases mentioned in the ANSI/AAMI Standard, a synthetic signal was generated to test all possible scenarios.

## 6.2.1 ANSI/AAMI EC13:2002

### Heart Rate error estimation

The standard establishes that the maximum error of the heart rate estimation must be  $\pm 5$ bpm or  $\pm 10\%$  of the original heart rate. Also, the heart rate range must be between 30 bpm and 200 bpm for adults.

### Delay on Alarms

The standard states that the maximum delay to alert tachycardia and bradycardia is 10 seconds. For the delay time of the diagnosis algorithm, it is necessary to simulate a heart rate of 80 bpm (Normal Sinus Rythm) and suddenly change the heart rate to 120 bpm, in the case of tachycardia. For bradycardia it is necessary to simulate a heart rate of 80 bpm and abruptly change it to 40 bpm. Finally, in the case of asystole, from the heart rate of 80 bpm the heart must suddenly stop. The delay time is calculated subtracting the time when the alarms activate and the time when the anomaly occurs. This experiment needs to be repeated 5 times. The mean delay has to be lower than 10 seconds and each experiment must not exceed 13 seconds.

## 6.2.2 Synthetic Signals

### Generation

The algorithm is based on [52] and [53] synthetic signal generation. Using a BCG beat reference, on entire BCG signal is created. The distance between J waves of the beats depends on the HR to be simulated. To avoid discontinuities of the signal, the latest 20 samples of the synthetic signal and the first 20 samples of BCG beat are summed with inverse weightings. Synthetic signals with HR of 30 to 300 BPM and the asystole case were created.

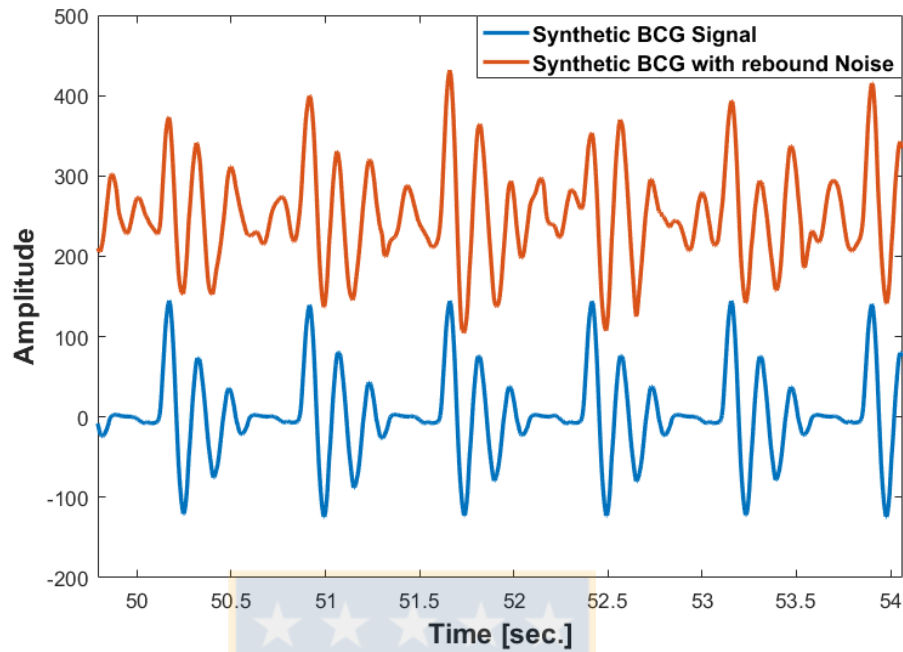


Figure 6.3: Noisy BCG Simulation. Synthetic clean BCG signal and the synthetic signal with rebound noise.

### Noise Simulation

In order to make a more realistic signal, two type of noise are added to the signal: respiration noise and rebound noise.

- **Respiration Noise:** It causes two effects: 1) A variation of the baseline of the BCG because the respiratory movements are detected by the sensors as changes in pressure. 2) The variation of amplitude of BCG beats, due to inspiration and expiration effects on the cardiac output.
- **Rebound Noise:** Is generated after the beat occurs due to its mechanical nature. Sometimes the amplitude of the rebound disrupts the signal and could be confused as heartbeat. Also, between beats, there is always some mechanical activity. To add this noise to the signal, each beat is multiplied with a Gaussian distribution window with a random skew, that can amplify the IJK wave or

amplify the rebound. Also, a mechanical noise, extracted from real signals is added to the baseline of the synthetic signal (Fig. 6.3).

Signals with these noises were simulated with different BCG-Respiration Ratio (16,8,4,0 and -4) and different BCG-Rebound Ratio (48,36,24,12,0 and -12) in order to calculate the robustness of the algorithm based on the standard (Eq. 6.1).

$$BCG - Noise \quad Ratio = 20 \cdot \log\left(\frac{RMS(BCG)}{RMS(Noise)}\right) \quad (6.1)$$





# Chapter 7

## Results

This chapter shows the results obtained from the diagnosis algorithm of cardiac activity, respiration activity and the SBC performance.

### 7.1 Cardiac Activity

#### 7.1.1 Position Accuracy

The subjects took 3 different postures, in order to evaluate the algorithm response. Two parameters were obtained: 1) the effective measure segments, which is the percentage of 15 seconds segment that was classified as clean over the total number of segments and 2) the HR error estimation, by calculating the mean error and SD error in 15 s windows from the BCG and the simultaneous ECG acquisition.

The algorithm has a lower HR error estimation when a subject is leaning on the backrest. Also, this leads to a lower number of discarded segments.

On a backrest posture, 51 % of effective measure segments was obtained, 26 % for sitting without backrest and 5.7 % when resting on thighs (Table 7.1).

Table 7.1: Number of discarded segments and HR error estimation for each position.

Positions	Total Segments	Segments discarded due to		Valid segments	HR error estimation	
		Correlation	Period SD		Mean	SD
Seat on backrest	1162	487	71	604	-0.41	1.88
Seat without backrest	1144	734	104	306	-0.05	2.82
Seat on thighs	1138	1057	15	66	1.21	5.07

Table 7.2: Noise Detection Accuracy

Total Noise Segment	Detected		Accuracy
	SD Periods	Correlations	
1725	36	1603	0.95

### 7.1.2 Noise Detection Accuracy

Noisy segments of 15 seconds were extracted from the activity sequence performed by the subjects (talking, movements of legs, head and arms). The total number of noisy segments was 1725, and 1639 were classified as noise by the diagnosis algorithm, which results in an accuracy of 0.95 (Table 7.2).

### 7.1.3 Diagnosis Accuracy

For relaxed and after exercise conditions, every clean BCG segment of 15 seconds was classified as a tachycardia, bradycardia, normal HR or asystole event. Also, each segment of 15 s of ECG is classified using the same criteria, in order to compare the diagnosis results between BCG and ECG. Using the ECG diagnoses as gold standard, the sensitivity ( $Se$ ) and positive predictive value ( $+P$ ) for each event is obtained. In a relaxed condition, the algorithm has a  $Se$  of 0.9 for tachycardia, 0.94 for bradycardia and 0.89 for normal HR. Also the  $+P$  value for tachycardia is 0.31, for bradycardia 0.82 and for normal HR 0.99, giving a general accuracy of 89.7% (Table 7.3).

Table 7.3: Diagnosis Accuracy: Resting Condition

	$T_{BCG}$	$B_{BCG}$	$N_{BCG}$	$A_{BCG}$	Total	Se
$T_{ECG}$	<b>19</b>	0	2	0	21	<b>0.90</b>
$B_{ECG}$	0	<b>61</b>	4	0	65	<b>0.94</b>
$N_{ECG}$	43	13	<b>462</b>	0	518	<b>0.89</b>
$A_{ECG}$	0	0	0	<b>0</b>	0	—
Total	62	74	468	0	<b>604</b>	
P+	<b>0.31</b>	<b>0.82</b>	<b>0.99</b>	—		

Table 7.4: Diagnosis Accuracy: After Exercise Condition

	$T_{BCG}$	$B_{BCG}$	$N_{BCG}$	$A_{BCG}$	Total	Se
$T_{ECG}$	<b>104</b>	0	12	0	116	<b>0.90</b>
$B_{ECG}$	1	<b>24</b>	5	0	30	<b>0.80</b>
$N_{ECG}$	27	9	<b>188</b>	0	224	<b>0.84</b>
$A_{ECG}$	0	0	0	<b>0</b>	0	—
Total	132	33	205	0	<b>370</b>	
P+	<b>0.79</b>	<b>0.73</b>	<b>0.92</b>	—		

For after exercise conditions, the  $Se$  to detect tachycardia is 0.9, for bradycardia 0.8 and for normal HR 0.84. The  $+P$  value is 0.79 for tachycardia, 0.73 for bradycardia and 0.92 for normal HR, giving a general accuracy of 85.4% (Table 7.4). No cases of asystole are recorded.

For the hospital measurements, the accuracy of the algorithm to detect heart rate abnormalities is calculated. Each 15 s segment of BCG and ECG is classified as an irregular (I) or regular (R) heart rate variability event. The  $Se$  for regular rhythm is 0.67 and for irregular rhythm is 0.78. The  $+P$  value for regular rhythm is 0.68 and for irregular rhythm is 0.77, giving a general accuracy of 73% (Table 7.5).

Table 7.5: Diagnosis Accuracy: Atrial Fibrillation

	$R_{BCG}$	$I_{BCG}$	Total	Se
$R_{ECG}$	<b>34</b>	17	51	<b>0.67</b>
$I_{ECG}$	16	<b>56</b>	72	<b>0.78</b>
Total	50	73	<b>123</b>	
P+	<b>0.68</b>	<b>0.77</b>		

## 7.1.4 Simulations Results

### HR error estimation

With BCG-Respiration Ratio value of -4 and BCG-Rebound Ratio value of 48, the algorithm obtains a maximum estimation error of -1.016 BPM at 160 BPM (Table 7.6) which meets the standard. In general, HR error estimation for all range of frequencies with the worst case of BCG-Respiration Ratio (-4), the algorithm starts to increase the error estimation from BCG-Rebound ratio of 12, being -12 the worst case, classifying all segments as noise (Table 7.7).

### Delay

Using the worst case of BCG-Respiration ratio (-4 dB), and the BCG-Rebound ratios of 48, 36, 24, 12, 0 and -12 dB, the delay alarm is calculated for the following cases: normal HR to tachycardia (N-T), normal HR to bradycardia (N-B) and normal HR to asystole (N-A).

The results show that the algorithm satisfies the standard alarm delay in all cases of noise for N-A. For N-B case, the algorithm reports alarms out of the allowed time range, and for BCG-Rebound ratio of 0 and -12 dB, it does not report any alarms at all. For N-T, the algorithm reports good results from BCG-Rebound ratios of 48 to 12 dB. Then, it reports alarms out of the allowed time range for 0 dB, and for -12 dB it does not report any alarm (Table 7.8).

Table 7.6: HR error of each frequency. HR error estimation of each frequency in the best case of noise.

BPM	Mean Error	SD Error
30	0.0011	0.011
40	0.0099	0.13
60	-0.0011	0.019
80	-0.0013	0.03
100	-0.0026	0.045
120	0.0013	0.039
140	0.0034	0.053
160	-0.0992	0.42
180	0.0052	0.052
200	-0.0056	0.077
220	0.0069	0.074
240	-0.022	0.083
260	-0.003	0.062
280	-0.058	0.083
300	-0.037	0.088

Table 7.7: General HR error estimation. For the worst case of BCG-Respiration ratio (-4) and for different levels of BCG-Rebound Ratio the error was calculated.

		HR estimation error	
		Mean	SD
BCG-Rebound Ratio	48	-0.0068	0.0637
	36	-0.0616	0.2971
	24	-0.1621	0.4994
	12	-3.3421	4.8258
	0	-21.4769	14.8927
	-12	—	—

## 7.2 Respiration Activity

### 7.2.1 Noise Detection Results

Similar to the BCG measurements, the respiration measurements of the lab were divided in two groups: 1) the clean respiration signals coming from resting activity,

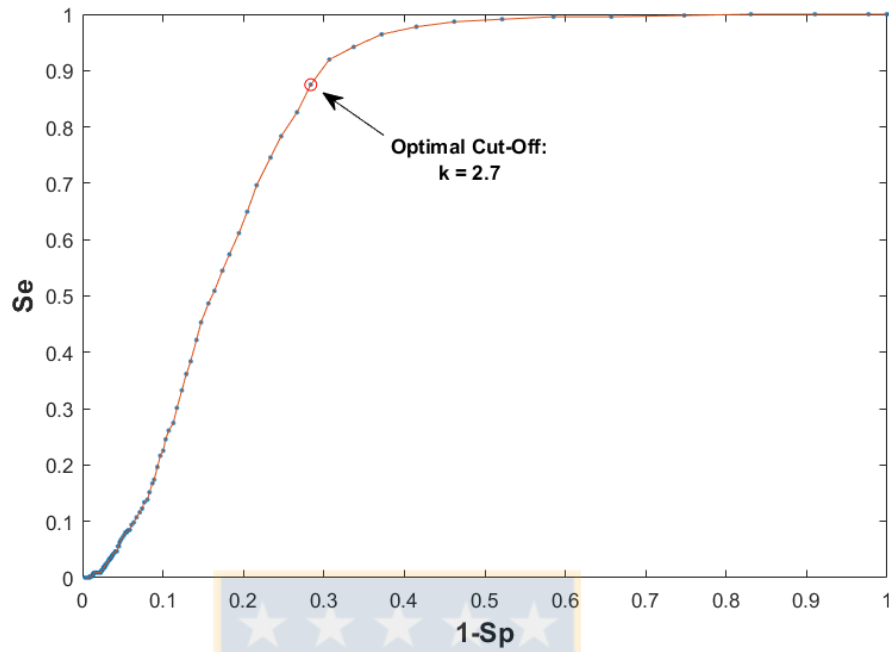


Figure 7.1: ROC curve of noisy respiration detection using different values of kurtosis

and 2) the noisy respirations signal coming from the sequence activity. Each group has segments of 30 seconds.

Different levels of kurtosis were used for classifying the segments in clean or noisy signal respiration. A Receiver Operating Characteristic or ROC curve was used to

Table 7.8: Delay simulation [sec.] for three cases: Normal HR to asystole, normal HR to bradycardia and normal HR to tachycardia for different levels of rebound noise.

		Normal HR to asystole		Normal HR to bradycardia		Normal HR to tachycardia	
		Mean	Max	Mean	Max	Mean	Max
BCG-Rebound Ratio	48	6.24	9.68	16.50	22.33	8.49	10.45
	36	7.40	9.63	15.65	21.24	8.19	11.00
	24	7.60	10.00	14.22	18.96	7.98	10.99
	12	7.53	9.69	20.12	22.26	8.29	10.44
	0	8.27	10.53	—	—	44.16	46.94
	-12	8.19	10.71	—	—	—	—

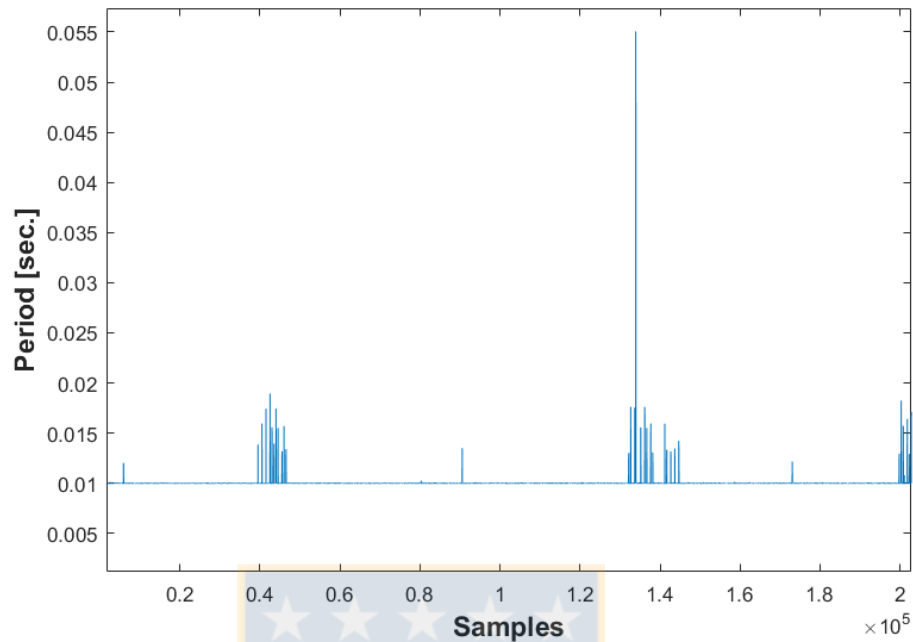


Figure 7.2: Timing Analysis of periods samples. It is not constant because is not a dedicated system. The rate of correct period sample is 99.9%.

analyse the performance of this classifier (Fig. 7.1). A kurtosis value of 2.7 has the best results, with a sensitivity of 0.875 and a specificity of 0.716.

### 7.2.2 Apnea Detection

The respiration diagnosis algorithm has a sensitivity of 0.86 and a positive predictive value of 0.76 for detecting stopped breathing.

## 7.3 Raspberry Performance

The real-time algorithms were run in a Raspberry Pi 3. Several performance indicators were measured to confirm that the system is able to process the data, such as: % CPU usage, % Memory usage, temperature and power requirements.

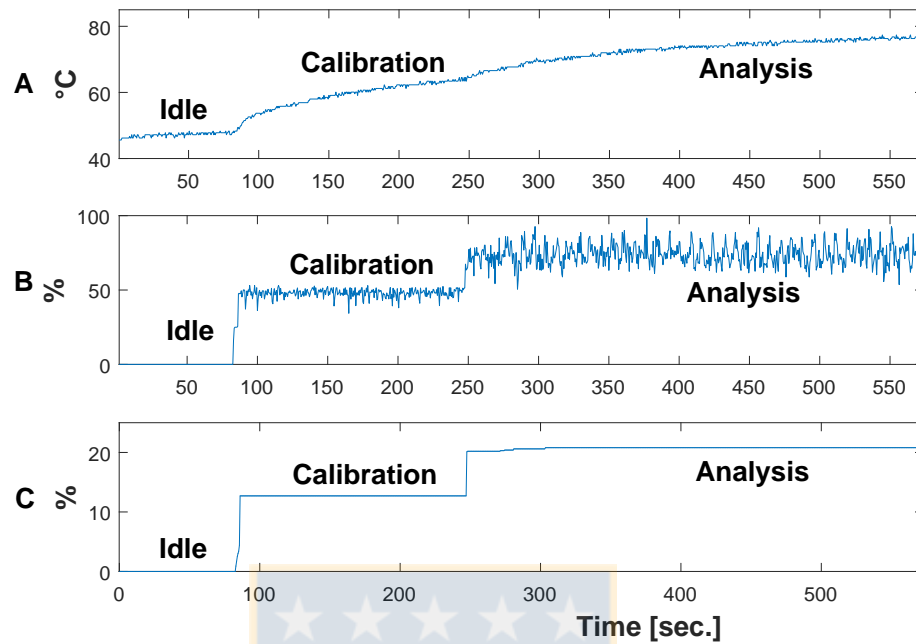


Figure 7.3: Raspberry Resources. **A:** Temperature, **B:** % CPU usage and **C:** % Memory usage.

### 7.3.1 Timing analysis

The BCG and respiratory algorithm needs less than 5 seconds for analysing segments. This means that it is possible to analyse signals with an overlap of 5 and 10 seconds respectively. Regarding the sampling frequency, it has variations because the SBC is not a dedicated system (Fig. 7.2).

### 7.3.2 Temperature

The maximum temperature reported was 77.4  $^{\circ}\text{C}$  using a heat sink. And the minimum temperature (in idle mode) was 45.6  $^{\circ}\text{C}$  (Fig. 7.3-A). A heat sink was used because the Raspberry Pi 3 reports a heating alarm during the analysis stage.



### 7.3.3 CPU usage

The complete algorithm is composed by 5 different processes: 1) Acquisition and calibration process, 2) WiFi communication process, 3) BCG signal algorithm process, 4) Respiration algorithm process and 5) Variable Manager process.

During the calibration mode, the main CPU usage is 47.85% with a peak value of 53.08%. After calibration, the main CPU usage is 74.08% with a peak value of 98.35%. The use of the 4 cores corresponds to 100% (Fig. 7.3 - B).

### 7.3.4 Memory usage

Signals acquired are stored temporally in RAM, with other static variables, functions and libraries from the different processes during their execution. The maximum amount of physical RAM used is 20.8 % of 1GByte RAM Memory. The algorithm was programmed to free the oldest data while new data are coming, in order to use

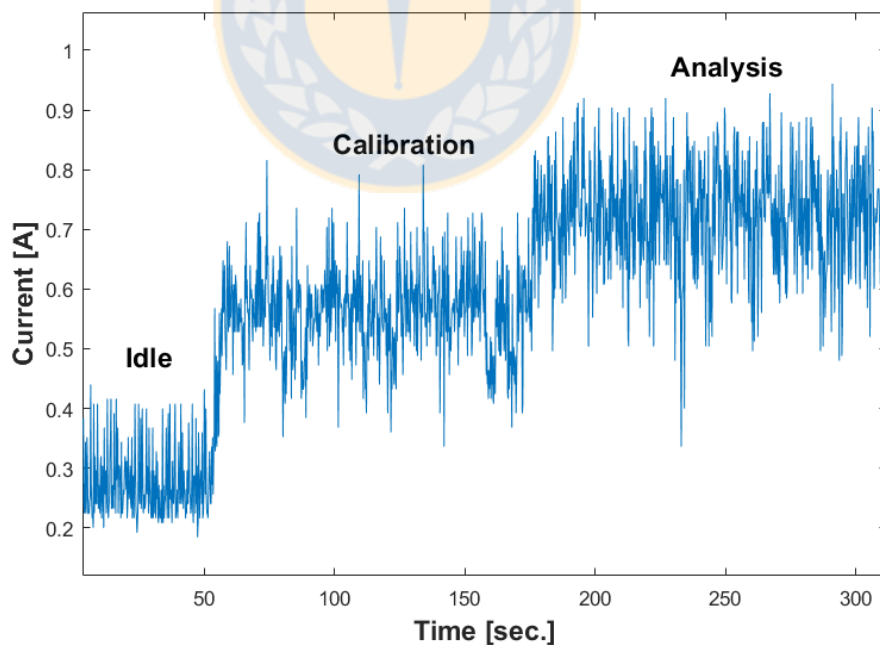


Figure 7.4: Raspberry current demand during algorithm execution.

the RAM efficiently. This is demonstrated by observing that the RAM usage remains constant (Fig. 7.3 - C).

### 7.3.5 Power Requirements

Raspberry consumes a mean current of 0.27 A in idle mode (all processes are turn off). With WiFi on, the mean demand of current increases to 0.3 A. During calibration stage the mean current increases to 0.63 A. Finally, during the analysis stage the mean increases to 0.78 A. All this calculations include the current needed to supply the analog circuit (Fig. 7.4).



# Chapter 8

## General Discussion and Conclusions

### 8.1 Discussion

The proposed system is able to measure cardiac and respiratory activity in a non-invasive way and to process them to obtain HR, HRV and RR to trigger alarms using the diagnostic algorithms.

One of the main limitations are the sensors themselves that capture the cardiac and respiratory signals. They do not respond equally to different pressure distributions. In light of this limitation, algorithms were developed to estimate the signals quality using correlation, the variability thresholds of the heart periods for the BCG, and the use of kurtosis for the respiratory signals. The advantage of these methods is that they are independent of the signal amplitude. This makes them respond better to changes in the signal amplitude, which does not necessarily imply noise, but an increased cardiac output or breathing deeper. The correlation method showed a good performance of 95% for noise detection, however, it also discards more than half of the clean segments due to its high sensitivity.

For different postures on the chair, the noise algorithm discarded different amounts

of segments. The best posture was being seated leaning on the backrest, because it has greater effective time of measurement, and it has an smallest average HR error. For this reason, this posture is recommended for measurements and monitoring.

Another important point is that the effectiveness of the algorithms depends on the calibration that has been done. From this stage, thresholds values to the respiration and BCG algorithms are obtained. It is recommended to instruct the subject to stay still (while monitored), in order to make a good calibration. Considering that a sitting person changes position many times, the effective measurement time would decrease.

Regarding the acquisition system, the SCB is not a dedicated hardware since it must carry out multiple processes in parallel, that may cause problems during signal acquisition. This issue affects the sampling frequency, leading problems to for the digital filters, that are configured at a fixed sampling frequency. Real-time operating systems have been developed for these devices, which could solve this problem.

The presence of false positives or false negatives is compensated by the mean in the BCG segments. However, for the last 5 seconds of the segment, the presence of false detections may not be compensated because the lower number of cardiac periods, giving false alarms due this criterion.

Regarding the simulations, the system is able to measure a HR range between 30 and 300 bpm. Even if they are not real cases, it is a good tool for observing how the algorithm responds. Other works have a limited HR range, not meeting the standard [54] [52] and they do not mention what happens when the signal is out of range.

With respect to the computational resources used to execute the algorithms, the Raspberry Pi 3 is able to perform the monitoring in real time. However, its current demand increases when the algorithm processes are active, increasing the CPU temperature. This can affect the CPU performance, so a ventilation system is needed to solve this problem.

This work is oriented to be economically accessible to the hospitals and homes.

Table 8.1: Material Costs

	Components	Unit Price \$USD	Quantity	Enterprice	Total Value \$USD
Sensors	EMFi	\$100	1	EMFIT	\$100
	PVDF	\$42.5	2	Images SI	\$85
	FSR	\$20.95	2	Sparkfun	\$41.9
Analog Circuit	PCB	\$16.61	1	OSH-Park	\$16.61
	ADC	\$6.61	1	RS-UK	\$6.61
	Digital Pot.	\$2.29	1	RS-UK	\$2.29
	Op. Amplifier	\$0.98	6	RS-UK	\$5.88
	Charge Pump	\$3	1	RS-UK	\$3
	RC Components	\$0.02	50	RS-UK	\$1
	Connectors	\$15	1	Victronics	\$15
SBC	Raspberry Pi 3	\$39.95	1	Sparkfun	\$39.95
	uSD Kingstone	\$8.95	1	Sparkfun	\$8.95
<b>TOTAL</b>					<b>\$326.19</b>

An estimate of the material cost to manufacture the system was calculated. The total cost is USD \$326.19 (Table 8.1). In addition, the place where it will be used must have access to a WiFi network in order to send the reports, which increases the cost. A market study would be needed to estimate the total cost and assess whether it is affordable.

## 8.2 Conclusions

The proposed monitoring system is capable of generating alarms from signals obtained using non-invasive sensors.

The proposed algorithm calculates heart rate with high accuracy and precision, however, it may be refined to achieve a longer effective measurement time.

Heart rate (tachycardia and bradycardia) alarms show better results than heart rate irregularity alarms.

The noise detection criteria for the BCG and respiration signals have good performance and are independent of signal amplitude, but should be improved with the

aim of reducing false alarms.

The Raspberry Pi SCB meets the requirements for real-time signal analysis and is a low-cost alternative for system development.



# Chapter 9

## Discusión General y Conclusiones

### 9.1 Discusión

El sistema propuesto es capaz de medir la actividad cardíaca y respiratoria de manera no invasiva y de procesarlas para obtener HR, HRV y RR para generar alarmas con los algoritmos de diagnóstico descritos.

Una de las principales limitaciones son los propios sensores que capturan las señales cardíaca y respiratoria, ya que estos no responden igualmente a diferentes distribuciones de presión. En vista a esta limitación, se desarrollaron algoritmos para estimar la calidad de las señales utilizando la correlación y los umbrales de variabilidad de los períodos cardíacos, para el caso del BCG y el uso de kurtosis para las señales respiratorias. La ventaja de estos métodos es que son independientes de la amplitud de la señal, lo que los hace responder mejor a los cambios en la amplitud de la señal, la que no necesariamente implican ruido, como el aumento del gasto cardíaco o una respiración más profunda. El método de correlación mostró un buen rendimiento de 95 % para la detección de ruido, sin embargo, también descarta más de la mitad de los segmentos limpios debido a su alta sensibilidad.

Para diferentes posturas en la silla, el algoritmo de ruido descartó diferentes cantidades de segmentos. La mejor postura fue la de estar sentado apoyado en el respaldo,

ya que obtuvo un mayor tiempo efectivo de medición y un error medio de HR menor que las otras posturas. Por esta razón, esta postura se recomienda para mediciones y monitoreo.

Otro punto importante es que la eficacia de los algoritmos depende de la calibración que se haya hecho, debido a que a partir de esta etapa se estiman los valores umbrales de los algoritmos de respiración y BCG. Sería recomendable instruir al sujeto a quedarse quieto (mientras es monitoreado) para realizar una buena calibración. Teniendo en cuenta que una persona sentada cambia de posición muchas veces, el tiempo de medición efectiva disminuiría.

Con respecto al sistema de adquisición, el SCB no es un hardware dedicado, ya que debe llevar a cabo múltiples procesos en paralelo, lo que podría provocar problemas durante la adquisición de señales. Por esto es que la frecuencia de muestreo se ve afectada, lo que a su vez afecta el uso de filtros digitales, que se configuran a una frecuencia de muestreo fija. Se han desarrollado sistemas operativos en tiempo real para estos dispositivos, lo que podría resolver este problema.

La presencia de falsos positivos o falsos negativos se compensa con la media en los segmentos BCG. Sin embargo, durante los últimos 5 segundos del segmento la presencia de falsas detecciones puede no ser compensada por el menor número de períodos cardiacos, dando falsas alarmas debido a este criterio.

Con respecto a las simulaciones, el sistema es capaz de medir un rango de HR entre 30 y 300 bpm. Si bien no son casos reales, es una buena herramienta para observar cómo responde el algoritmo. Otros algoritmos propuestos tienen rango de HR limitado y no cumplen con el estándar [54] [52]. Además, no mencionan lo que sucede cuando el HR de la señal está fuera de rango que pueden medir.

Con respecto a los recursos computacionales utilizados para ejecutar los algoritmos, el Raspberry Pi 3 es capaz de realizar el monitoreo en tiempo real. Sin embargo, su demanda de corriente aumenta cuando los procesos del algoritmo están activos, aumentando la temperatura de la CPU. Esto puede afectar el rendimiento de ésta,



Table 9.1: Costos de los materiales

	Componentes	Precio Unitario \$USD	Cantidad	Empresa	Valor Total \$USD
Sensores	EMFi	\$100	1	EMFIT	\$100
	PVDF	\$42.5	2	Images SI	\$85
	FSR	\$20.95	2	Sparkfun	\$41.9
Circuito Analógico	PCB	\$16.61	1	OSH-Park	\$16.61
	ADC	\$6.61	1	RS-UK	\$6.61
	Pot. Digital	\$2.29	1	RS-UK	\$2.29
	Amplificador	\$0.98	6	RS-UK	\$5.88
	Bomba Carga	\$3	1	RS-UK	\$3
	Componentes RC	\$0.02	50	RS-UK	\$1
	Conectores	\$15	1	Victronics	\$15
SBC	Raspberry Pi 3	\$39.95	1	Sparkfun	\$39.95
	uSD Kingstone	\$8.95	1	Sparkfun	\$8.95
<b>TOTAL</b>					<b>\$326.19</b>

por lo que se necesita un sistema de ventilación para resolver este problema.

Este trabajo está orientado a ser económicamente accesible a los hospitales y hogares. Para ello, se calculó una estimación del costo material para fabricar el sistema. El costo total es USD \$326.19 (Tabla 9.1). Además, el lugar donde se va a utilizar debe tener acceso a una red WiFi para enviar los reportes, lo que aumenta el costo. Un estudio de mercado sería necesario para estimar el costo total y evaluar si es asequible.

## 9.2 Conclusiones

El sistema de monitoreo propuesto es capaz de generar alarmas a partir de señales obtenidas utilizando sensores no invasivos.

El algoritmo propuesto calcula la frecuencia cardíaca con alta exactitud y precisión, sin embargo, podría ser mejorada para lograr un mayor tiempo de medición efectivo.

Las alarmas de frecuencia cardíaca (taquicardia y bradicardia) muestran mejores

resultados que las alarmas de irregularidad cardíaca.

Los criterios de detección de ruido para las señales BCG y de respiración tienen un buen rendimiento y son independientes de la amplitud de la señal, pero deben mejorarse con el objetivo de reducir las falsas alarmas.

El SCB Raspberry Pi cumple con los requisitos para el análisis de señales en tiempo real y es una alternativa de bajo costo para el desarrollo del sistema.



# Chapter 10

## Publications

### 10.1 ISI Paper Submitted

**Javier A.P. Chávez**, Esteban J. Pino, Eduardo Lecannelier, Pablo Aqueveque, “Non-Obtrusive System for Monitoring Cardiac Activity”, Submitted to the Journal of IEEE Transactions on Biomedical Engineering. March 2017.

### 10.2 Conferences

- Esteban J. Pino, Constanza Larsen, **Javier Chávez** and Pablo Aqueveque, “Non-Invasive BCG Monitoring for Non-Traditional Settings”, *38th Annual International Conference of the IEEE Engineering in Medicine and Biology Society*, Orlando 2016.
- Esteban J. Pino, **Javier A.P. Chávez**, Pablo Aqueveque, “Noninvasive Ambulatory Measurement System of Cardiac Activity”, *37th Annual International Conference of the IEEE Engineering in Medicine and Biology Society*, Milán 2015.
- Esteban J. Pino, **Javier A.P. Chávez**, Constanza Larsen, Carlos Villagrán,

Pablo Aqueveque, “Non-Invasive System for Ubiquitous Physiological Home Monitoring”, *Mobile and Information Technologies in Medicine and Health MobileMed*, 2014.

- **Javier A.P. Chávez**, Esteban J. Pino, “Non-Invasive System Proposal for Ambulatory Measurement during Sleep”, *International Student Conference Chile / 7th Biomedical Engineering Conference Universidad de Concepción*, 2014.



# Bibliography

- [1] Paul Kowal Wan He, Daniel Goodkind. An aging world: 2015. *International Population Reports, P95/16-1*, 2016.
- [2] Terra Chile. Hombre muere en sala de espera de hospital en calama. <https://noticias.terra.cl/chile/hombre-muere-en-sala-de-espera-de-hospital-en-calama,dc391079ac637410VgnVCM4000009bcceb0aRCRD.html>, Julio 2014. (Accessed on 01/04/2017).
- [3] Diario La Nación Noticias de Chile y el mundo. Sumario en hospital san José por muerte en sala de espera. <http://www.lanacion.cl/sumario-en-hospital-san-jose-por-muerte-en-sala-de-espera/noticias/2011-01-11/145111.html>, Enero 2011. Accessed on 01/04/2017.
- [4] BioBioChile. Mujer muere tras esperar por más de 10 horas en urgencia del hospital base de valdivia. <http://www.biobiochile.cl/noticias/2012/07/06/mujer-muere-tras-esperar-por-mas-de-10-horas-en-urgencia-del-hospital-base-de-valdivia.shtml>, Julio 2012. (Accessed on 01/04/2017).
- [5] TVN 24 horas. Investigan muerte de paciente en la sala de espera. <http://www.24horas.cl/regiones/araucania/araucania-investigan-muerte-de-paciente-en-la-sala-de-espera-1177439>, Abril 2014. (Accessed on 01/04/2017).
- [6] Dan Mihai Stefanescu. *Handbook of force transducers: principles and components*. Springer Science & Business Media, 2011.

- [7] Esteban J Pino, Astrid Dörner De la Paz, Pablo Aqueveque, Javier AP Chávez, and Alejandra A Morán. Contact pressure monitoring device for sleep studies. In *2013 35th Annual International Conference of the IEEE Engineering in Medicine and Biology Society (EMBC)*, pages 4160–4163. IEEE, 2013.
- [8] Diego E Arias, Esteban J Pino, Pablo Aqueveque, and Dorothy W Curtis. Unobtrusive support system for prevention of dangerous health conditions in wheelchair users. *Mobile Information Systems*, 2016.
- [9] Belén Cavallar Leiva. Sistema autónomo de recomendaciones para usuarios de silla de ruedas motorizada. B.S. thesis, Universidad de Concepción, Marzo 2016.
- [10] Fsr force sensing resistor integration guide and evaluation guides catalog. <https://www.sparkfun.com/datasheets/Sensors/Pressure/fsrguide.pdf>.
- [11] Satu Rajala and Jukka Lekkala. Film-type sensor materials PVDF and EMFi in measurement of cardiorespiratory signals—a review. *IEEE Sensors Journal*, 12(3):439–446, 2012.
- [12] Satu Rajala and Jukka Lekkala. PVDF and EMFi sensor materials—a comparative study. *Procedia Engineering*, 5:862–865, 2010.
- [13] Kyuichi Niizeki, Izumi Nishidate, Kazami Uchida, and Mikio Kuwahara. Unconstrained cardiorespiratory and body movement monitoring system for home care. *Medical and Biological Engineering and Computing*, 43(6):716–724, 2005.
- [14] Octavian Postolache, Pedro Silva Girao, Joaquim Mendes, and Gabriela Postolache. Unobtrusive heart rate and respiratory rate monitor embedded on a wheelchair. In *Medical Measurements and Applications, 2009. MeMeA 2009. IEEE International Workshop on*, pages 83–88. IEEE, 2009.
- [15] Juha M Kortelainen, Mark van Gils, and Juha Pärkkä. Multichannel bed pressure

- sensor for sleep monitoring. In *2012 Computing in Cardiology*, pages 313–316. IEEE, 2012.
- [16] Xin Zhu, Wenxi Chen, Tetsu Nemoto, Yumi Kanemitsu, Keiichiro Kitamura, and Kenichi Yamakoshi. Accurate determination of respiratory rhythm and pulse rate using an under-pillow sensor based on wavelet transformation. In *Annual International Conference of the IEEE Engineering in Medicine and Biology- Proceedings*, pages 5869–5872, 2005.
- [17] Alireza Akhbardeh, Sakari Junnila, Mikko Koivuluoma, Teemu Koivistoinen, and A Varri. The heart disease diagnosing system based on force sensitive chair’s measurement, biorthogonal wavelets and neural networks. In *Proceedings, 2005 IEEE/ASME International Conference on Advanced Intelligent Mechatronics.*, pages 676–681. IEEE, 2005.
- [18] Sonia Gilaberte, Joan Gómez-Clapers, Ramon Casanella, and Ramon Pallas-Areny. Heart and respiratory rate detection on a bathroom scale based on the ballistocardiogram and the continuous wavelet transform. In *2010 Annual International Conference of the IEEE Engineering in Medicine and Biology*, pages 2557–2560. IEEE, 2010.
- [19] O Postolache, P Silva Girao, G Postolache, and M Pereira. Vital signs monitoring system based on emfi sensors and wavelet analysis. In *2007 IEEE Instrumentation & Measurement Technology Conference IMTC 2007*, pages 1–4. IEEE, 2007.
- [20] Metin Akay. *Time Frequency and Wavelets in Biomedical Signal Processing*. IEEE Press series in biomedical Engineering, 1998.
- [21] Norden E Huang, Zheng Shen, Steven R Long, Manli C Wu, Hsing H Shih, Quan-nan Zheng, Nai-Chyuan Yen, Chi Chao Tung, and Henry H Liu. The empirical

- mode decomposition and the hilbert spectrum for nonlinear and non-stationary time series analysis. In *Proceedings of the Royal Society of London A: Mathematical, Physical and Engineering Sciences*, volume 454, pages 903–995. The Royal Society, 1998.
- [22] Byung Hun Choi, Gih Sung Chung, Jin-Seong Lee, Do-Un Jeong, and Kwang Suk Park. Slow-wave sleep estimation on a load-cell-installed bed: a non-constrained method. *Physiological measurement*, 30(11):1163, 2009.
- [23] Christoph Bruser, Kurt Stadlthanner, Stijn de Waele, and Steffen Leonhardt. Adaptive beat-to-beat heart rate estimation in ballistocardiograms. *IEEE Transactions on Information Technology in Biomedicine*, 15(5):778–786, 2011.
- [24] Oscar Hernandez, Carlos Ramirez, and Julio Villeda. A tolerant algorithm for cardiac pulses characterization in ballistocardiography signals in a non-invasive system. In *2011 IEEE Statistical Signal Processing Workshop (SSP)*, pages 465–468. IEEE, 2011.
- [25] JH Shin, BH Choi, YG Lim, DU Jeong, and KS Park. Automatic ballistocardiogram (bcg) beat detection using a template matching approach. In *2008 30th Annual International Conference of the IEEE Engineering in Medicine and Biology Society*, pages 1144–1146. IEEE, 2008.
- [26] Katy Lydon, Bo Yu Su, Licet Rosales, Moein Enayati, KC Ho, Marilyn Rantz, and Marjorie Skubic. Robust heartbeat detection from in-home ballistocardiogram signals of older adults using a bed sensor. In *2015 37th Annual International Conference of the IEEE Engineering in Medicine and Biology Society (EMBC)*, pages 7175–7179. IEEE, 2015.
- [27] Esteban J Pino, Constanza Larsen, Javier Chavez, and Pablo Aqueveque. Non-invasive bcg monitoring for non-traditional settings. In *Engineering in Medicine*



- and Biology Society (EMBC), 2016 IEEE 38th Annual International Conference of the*, pages 4776–4779. IEEE, 2016.
- [28] Esteban J Pino, Javier AP Chávez, and Pablo Aqueveque. Noninvasive ambulatory measurement system of cardiac activity. In *2015 37th Annual International Conference of the IEEE Engineering in Medicine and Biology Society (EMBC)*, pages 7622–7625. IEEE, 2015.
- [29] Po-Hsiang Lai and Insoo Kim. Lightweight wrist photoplethysmography for heavy exercise: motion robust heart rate monitoring algorithm. *Healthcare technology letters*, 2(1):6, 2015.
- [30] Wei Lu, Michelle M Nystrom, Parag J Parikh, David R Fooshee, James P Hubenschmidt, Jeffrey D Bradley, and Daniel A Low. A semi-automatic method for peak and valley detection in free-breathing respiratory waveforms. *Medical physics*, 33(10):3634–3636, 2006.
- [31] Liangyou Chen, Thomas McKenna, Andrew Reisner, and Jaques Reifman. Algorithms to qualify respiratory data collected during the transport of trauma patients. *Physiological measurement*, 27(9):797, 2006.
- [32] J Alametsä, J Viik, J Alakare, A Värri, and A Palomäki. Ballistocardiography in sitting and horizontal positions. *Physiological measurement*, 29(9):1071, 2008.
- [33] Abdul Qadir Javaid, Andrew D Wiens, Nathaniel Forrest Fesmire, Mary Ann Weitnauer, and Omer T Inan. Quantifying and reducing posture-dependent distortion in ballistocardiogram measurements. *IEEE journal of biomedical and health informatics*, 19(5):1549–1556, 2015.
- [34] Jae Hyuk Shin, Young Joon Chee, Do-Un Jeong, and Kwang Suk Park. Nonconstrained sleep monitoring system and algorithms using air-mattress with balanc-

- ing tube method. *IEEE transactions on information technology in biomedicine*, 14(1):147–156, 2010.
- [35] Rajet Krishnan, Balasubramaniam Natarajan, and Steve Warren. Analysis and detection of motion artifact in photoplethysmographic data using higher order statistics. In *2008 IEEE International Conference on Acoustics, Speech and Signal Processing*, pages 613–616. IEEE, 2008.
- [36] Omer T Inan, Pierre-Francois Migeotte, Kwang-Suk Park, Mozziyar Etemadi, Kouhyar Tavakolian, Ramon Casanella, John Zanetti, Jens Tank, Irina Funtova, G Kim Prisk, et al. Ballistocardiography and seismocardiography: A review of recent advances. *IEEE journal of biomedical and health informatics*, 19(4):1414–1427, 2015.
- [37] Markos G Tsipouras, Dimitrios I Fotiadis, and D Sideris. An arrhythmia classification system based on the rr-interval signal. *Artificial intelligence in medicine*, 33(3):237–250, 2005.
- [38] Anton Aboukhalil, Larry Nielsen, Mohammed Saeed, Roger G Mark, and Gari D Clifford. Reducing false alarm rates for critical arrhythmias using the arterial blood pressure waveform. *Journal of biomedical informatics*, 41(3):442–451, 2008.
- [39] Irena Jekova and Vessela Krasteva. Real time detection of ventricular fibrillation and tachycardia. *Physiological measurement*, 25(5):1167, 2004.
- [40] Nicole Burns. Cardiovascular physiology. *Retrieved from School of Medicine, Trinity College, Dublin*, 2013.
- [41] Paris B Lovett, Jason M Buchwald, Kai Stürmann, and Polly Bijur. The vexatious vital: neither clinical measurements by nurses nor an electronic monitor

- provides accurate measurements of respiratory rate in triage. *Annals of emergency medicine*, 45(1):68–76, 2005.
- [42] Javier Chávez Cerda. Sistema no invasivo de medición ambulatoria de variables fisiológicas. B.S. thesis, Universidad de Concepción, Marzo 2015.
- [43] Matthias Daniel Zink, Christoph Brüser, Patrick Winnersbach, Andreas Napp, Steffen Leonhardt, Nikolaus Marx, Patrick Schauerte, and Karl Mischke. Heart-beat cycle length detection by a ballistocardiographic sensor in atrial fibrillation and sinus rhythm. *BioMed research international*, 2015, 2015.
- [44] U Rajendra Acharya, K Paul Joseph, Natarajan Kannathal, Choo Min Lim, and Jasjit S Suri. Heart rate variability: a review. *Medical and biological engineering and computing*, 44(12):1031–1051, 2006.
- [45] Task Force of the European Society of Cardiology et al. Heart rate variability standards of measurement, physiological interpretation, and clinical use. *Eur Heart J*, 17:354–381, 1996.
- [46] Marek Malik. Time-domain measurement of heart rate variability. *Cardiac Electrophysiology Review*, 1(3):329–334, 1997.
- [47] Mary A Woo, William G Stevenson, Debra K Moser, Robert B Trelease, and Ronald M Harper. Patterns of beat-to-beat heart rate variability in advanced heart failure. *American heart journal*, 123(3):704–710, 1992.
- [48] Ary L Goldberger, Luis AN Amaral, Leon Glass, Jeffrey M Hausdorff, Plamen Ch Ivanov, Roger G Mark, Joseph E Mietus, George B Moody, Chung-Kang Peng, and H Eugene Stanley. Physiobank, physiotoolkit, and physionet components of a new research resource for complex physiologic signals. *Circulation*, 101(23):e215–e220, 2000.

- [49] George B Moody and Roger G Mark. A new method for detecting atrial fibrillation using RR intervals. *Computers in Cardiology*, 10(1):227–230, 1983.
- [50] Jiapu Pan and Willis J Tompkins. A real-time QRS detection algorithm. *IEEE transactions on biomedical engineering*, BME-32(3):230–236, 1985.
- [51] American National Standard (ANSI/AAMI EC13:2002). *Cardiac monitors, heart rate meters, and alarms*. Association for the Advancement of Medical Instrumentation, 2002.
- [52] Joonas Paalasmaa, Hannu Toivonen, and Markku Partinen. Adaptive heartbeat modeling for beat-to-beat heart rate measurement in ballistocardiograms. *IEEE journal of biomedical and health informatics*, 19(6):1945–1952, 2015.
- [53] Felipe I Donoso, Rosa L Figueroa, Eduardo A Lecannelier, Esteban J Pino, and Alejandro J Rojas. Atrial activity selection for atrial fibrillation ECG recordings. *Computers in biology and medicine*, 43(10):1628–1636, 2013.
- [54] Carlos Alvarado-Serrano, Pablo Samuel Luna-Lozano, and Ramon Pallàs-Areny. An algorithm for beat-to-beat heart rate detection from the BCG based on the continuous spline wavelet transform. *Biomedical Signal Processing and Control*, 27:96–102, 2016.